Earth and Planetary surfaces observation from optical methods

Jean-Philippe Avouac
California Institute of Technology

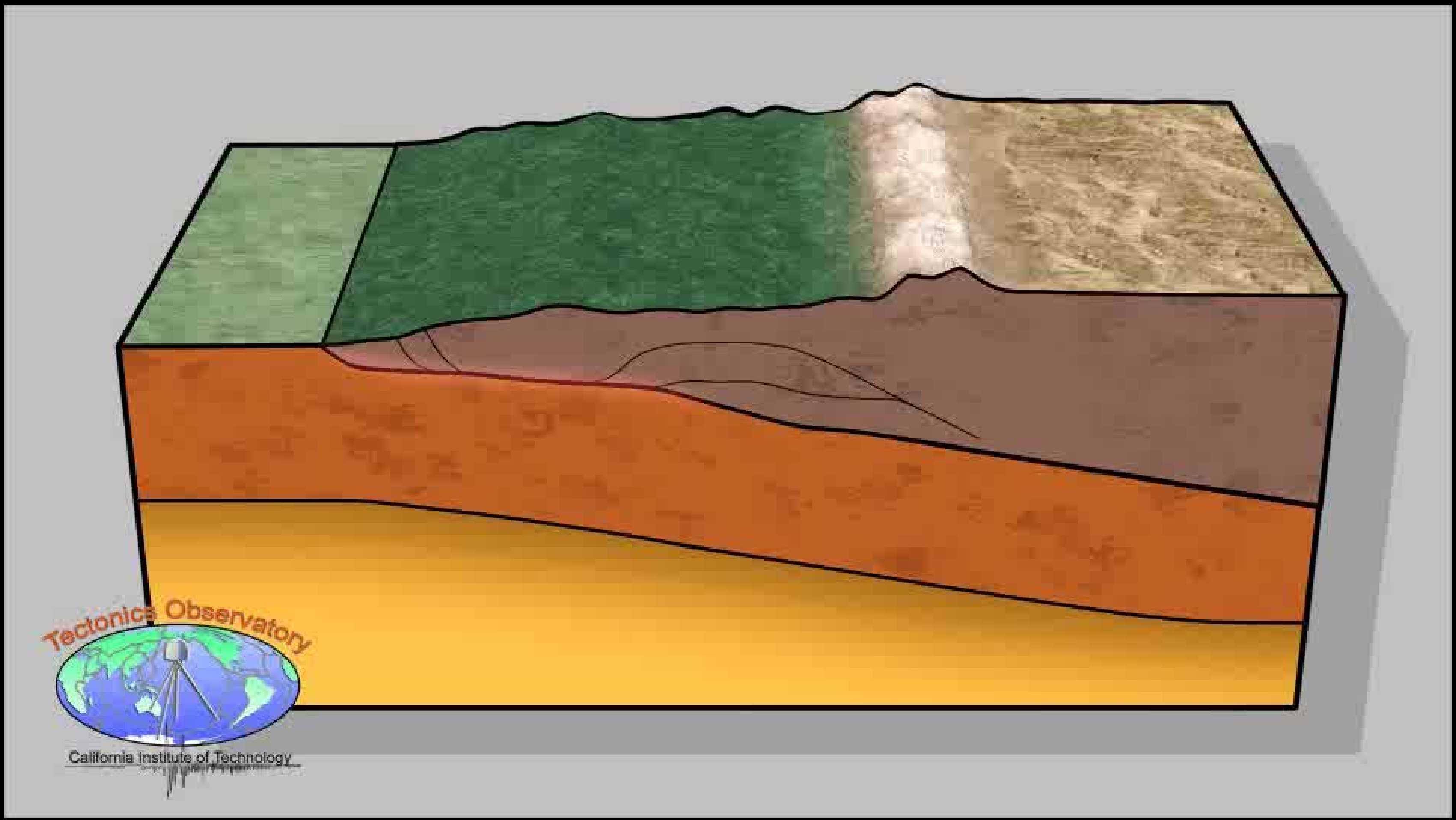
Tectonics Observatory
California Institute of Technology

Dynamic modeling of the seismic cycle

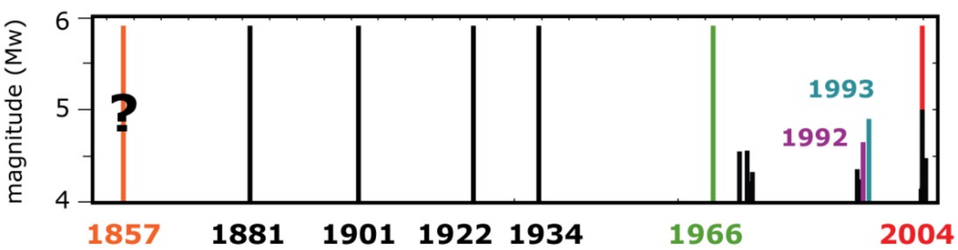

Modeling the Parkfield EQ Sequence on the SAF

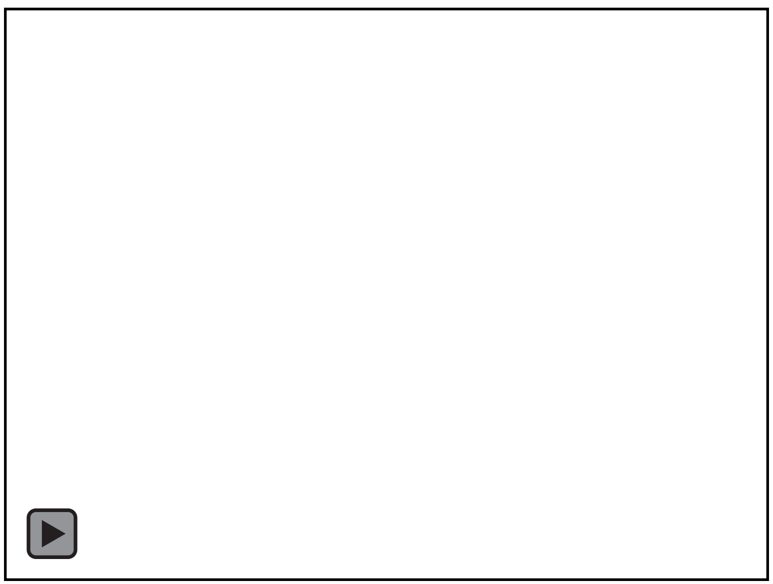

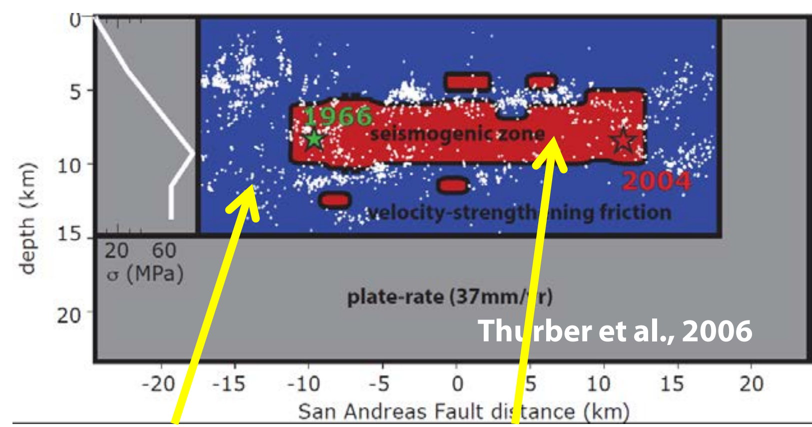

Rate Strengthening   Rate Weakening

(Barbot et al., 2012)

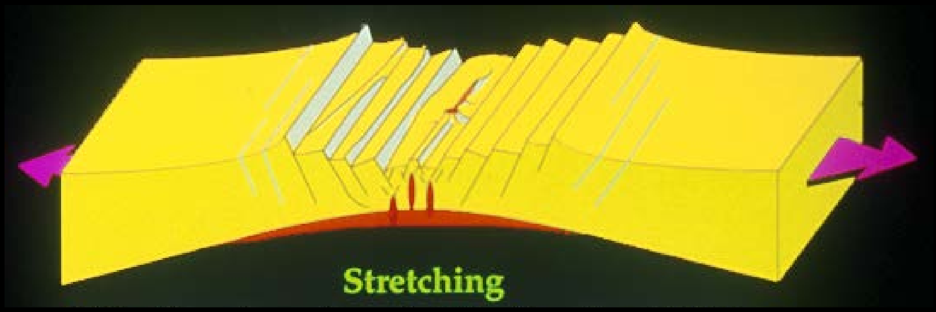

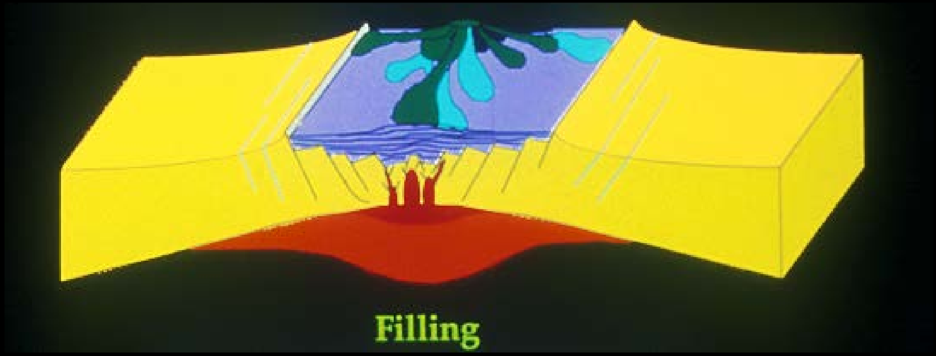

Tectonics Observatory
California Institute of Technology

Optical Remote Sensing

Passive

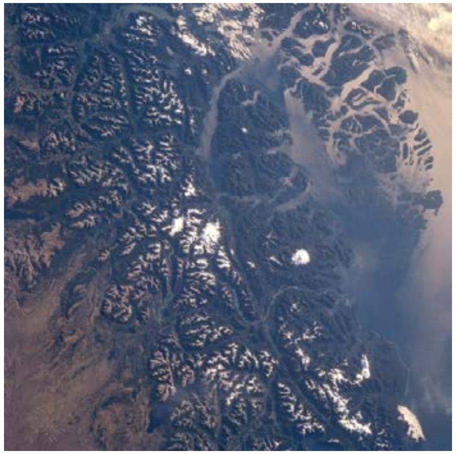

swath

Active

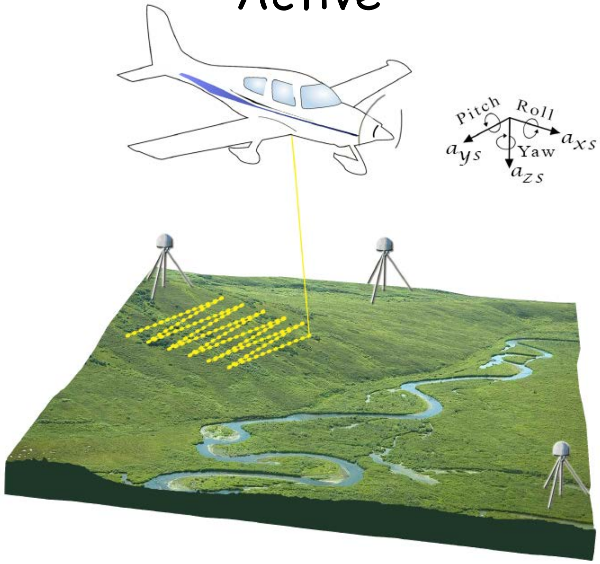

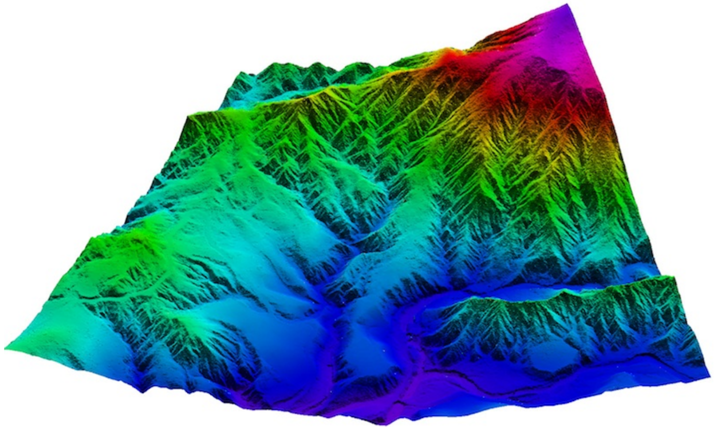

swath

Satellite	Spatial Resolution	Swath	Bands	Best Repeat Time	Stereo Capable
Landsat 8	15 – 100 m	185 km	Pan + 10 MS	16 days	No
SPOT 5	2.5 - 20m	60 km	Pan + 4 MS	3 days	No
SPOT 6 & 7	1.5 – 6 m	60 km	Pan + 4 MS	3 days	Yes
Worldview 1	0.5 m	17.6 km	Pan	1-6 days	Yes
Worldview 2	0.46 – 1.84m	16.4 km	Pan + 8 MS	1-6 days	Yes
Worldview 3	0.31 – 3.7m	13.1 km	Pan + 16 MS	1 day	Yes
Pleiades 1A & 1B	0.7 - 2.8m	20 km	Pan + 4 MS	3 days	Yes

Earth Observation from Space Optical Systems
- Some milestones -

- Landsat-1 to 7 (1970s): 30m GSD, 180km, nadir.
- SPOT1-4 (1980s): 10m GSD, 60km, steering.
- ASTER (2000): 15m, 60km, stereo.
- High Resolution Commercial systems(2000s): Quickbird, Ikonos, Worldview….
- Landsat-8 (2013): 15m GSD, 180km, nadir, global coverage,16 days repeat time.

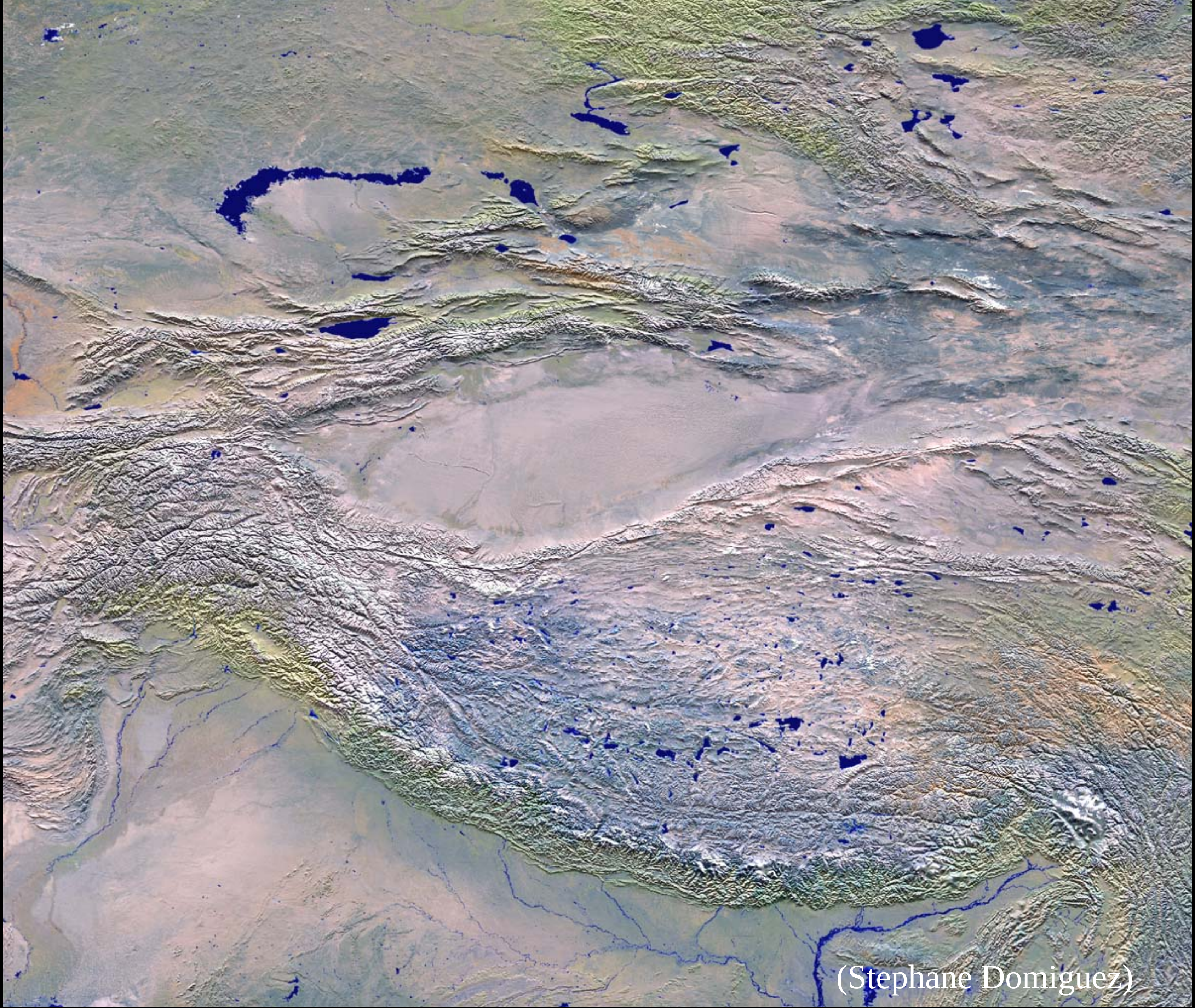
(Stephane Domiguez)

The Altyn Tagh Fault (Karakax Valley)

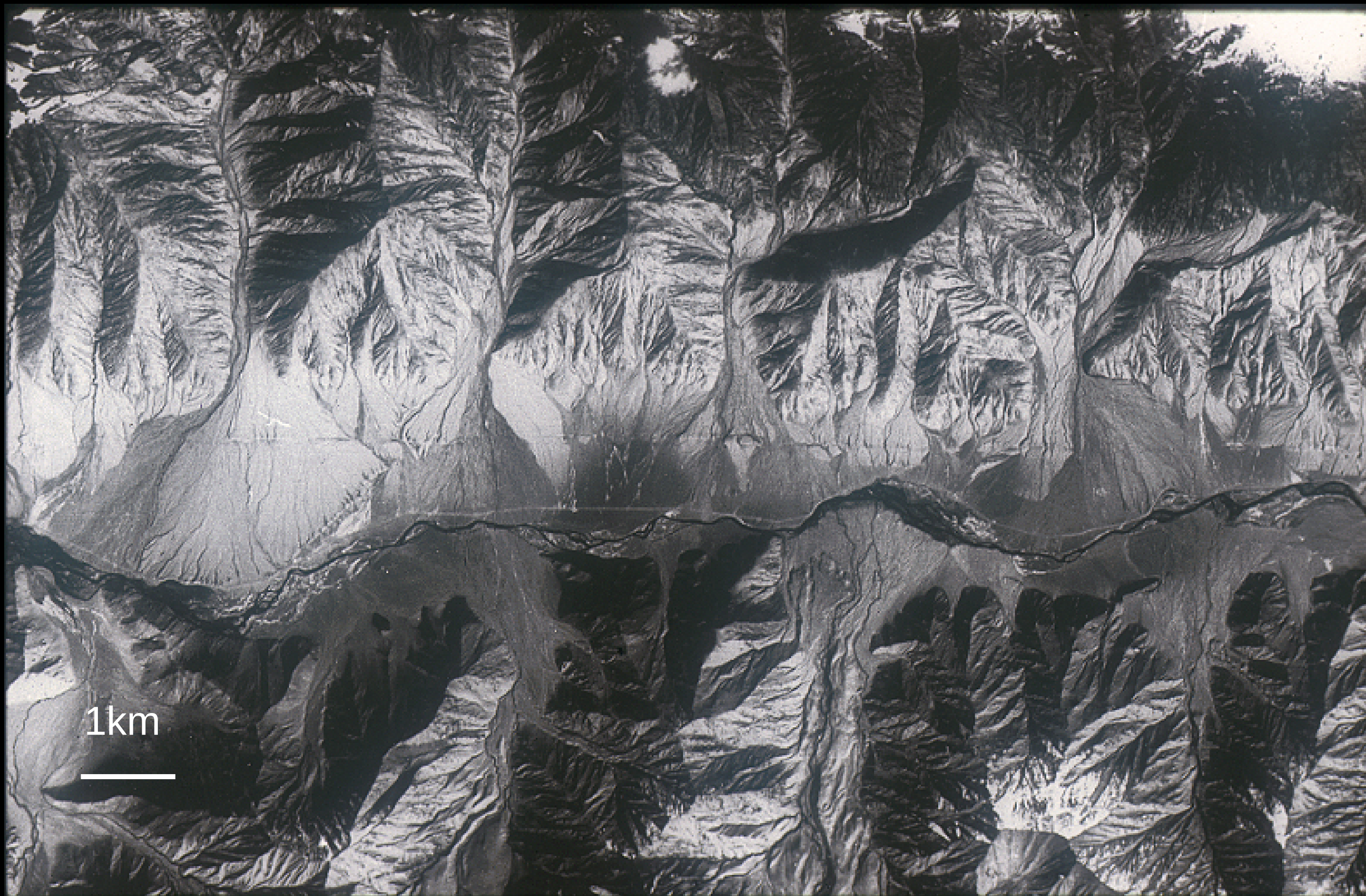

SPOT image (copyright CNES-1988)- Gilles Peltzer

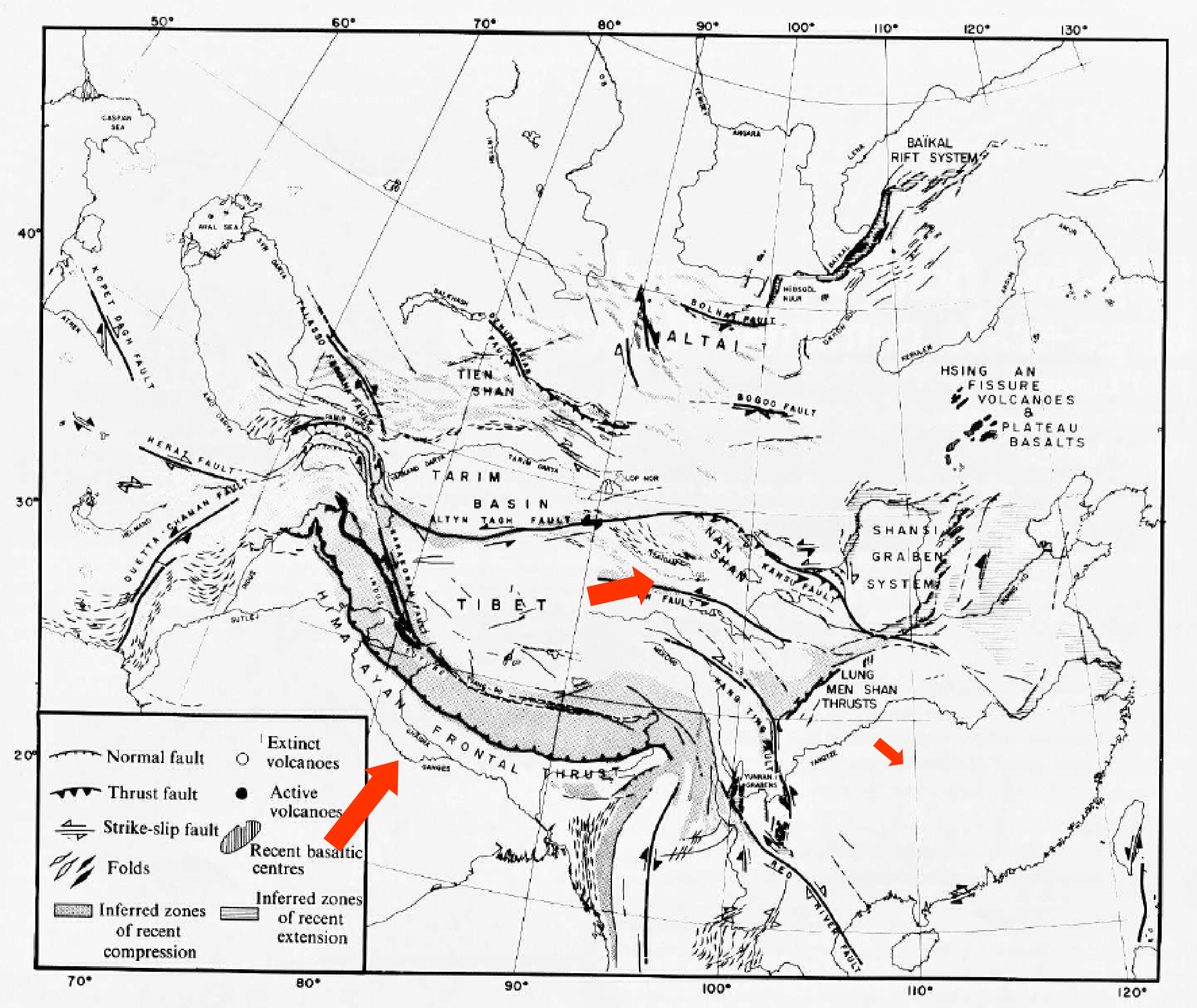

(Tapponnier and Molnar, 1975)

Altyn Tagh Fault SPOT Image-pixel size 10m- 10kmx7km

Offset terrace risers

155m

Offset terrace risers

Offset terrace risers

The Kunlun Fault

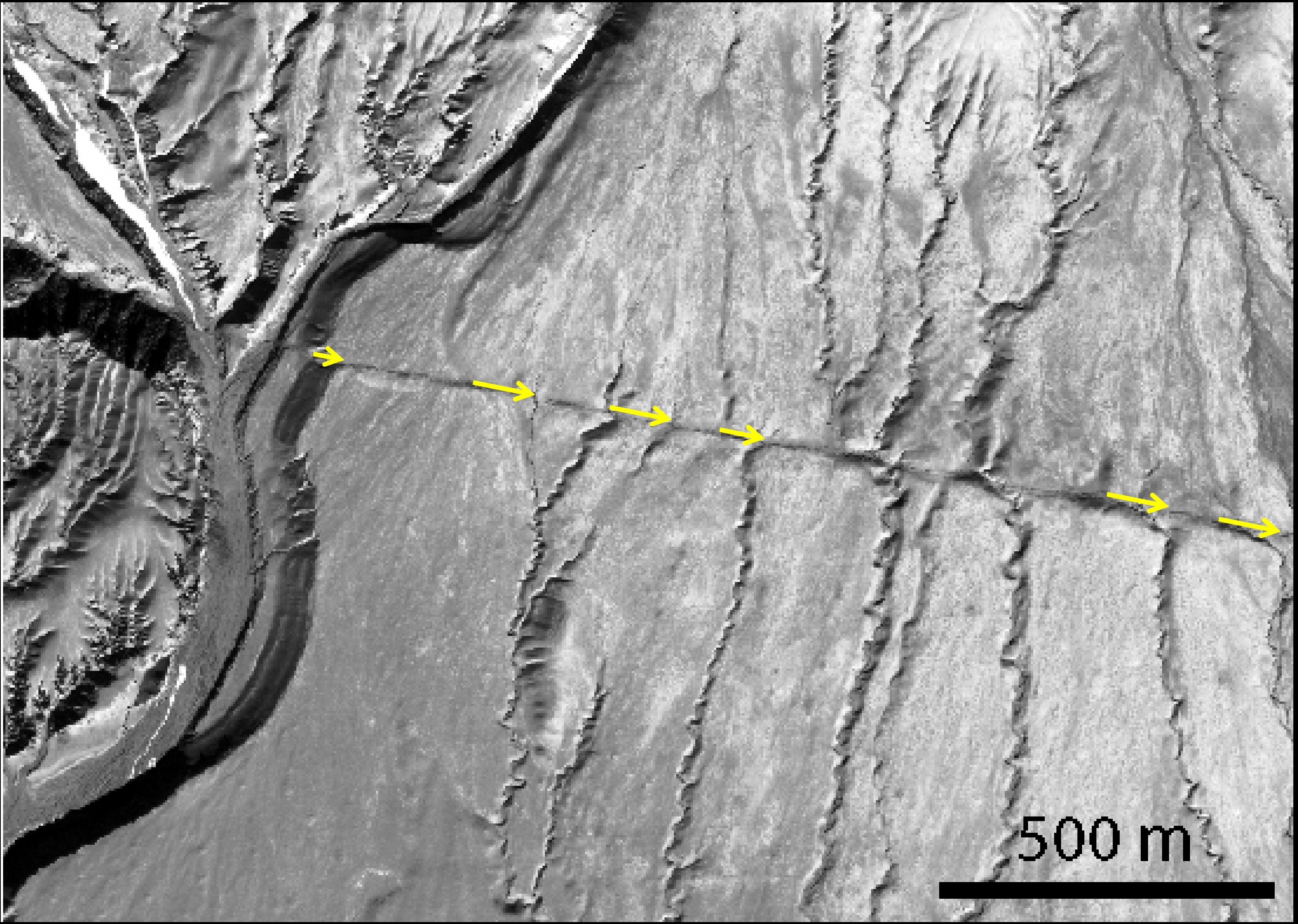

Van Der Woerd et al, (1998) - SPOT image, Copyright CNES-1988

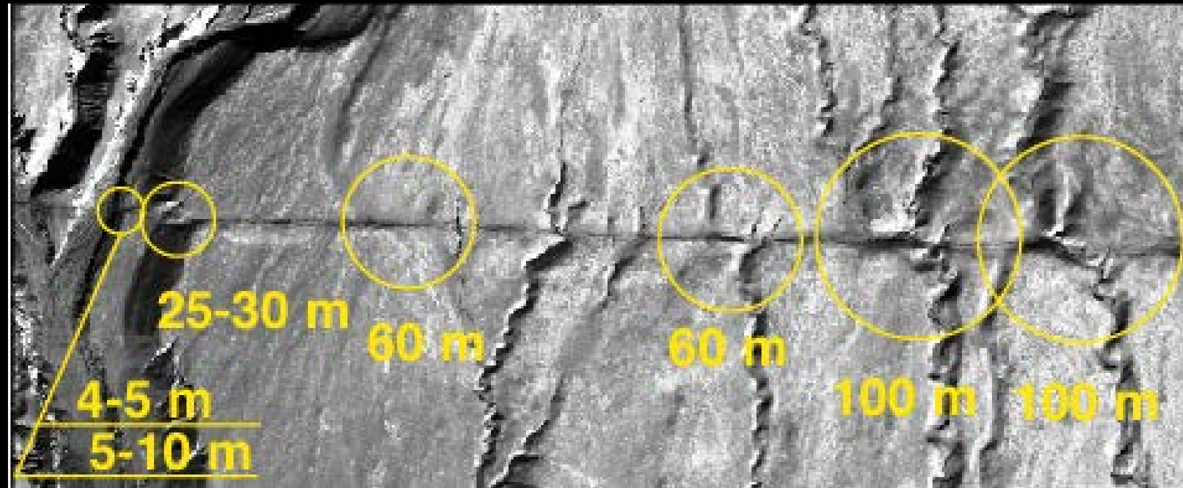

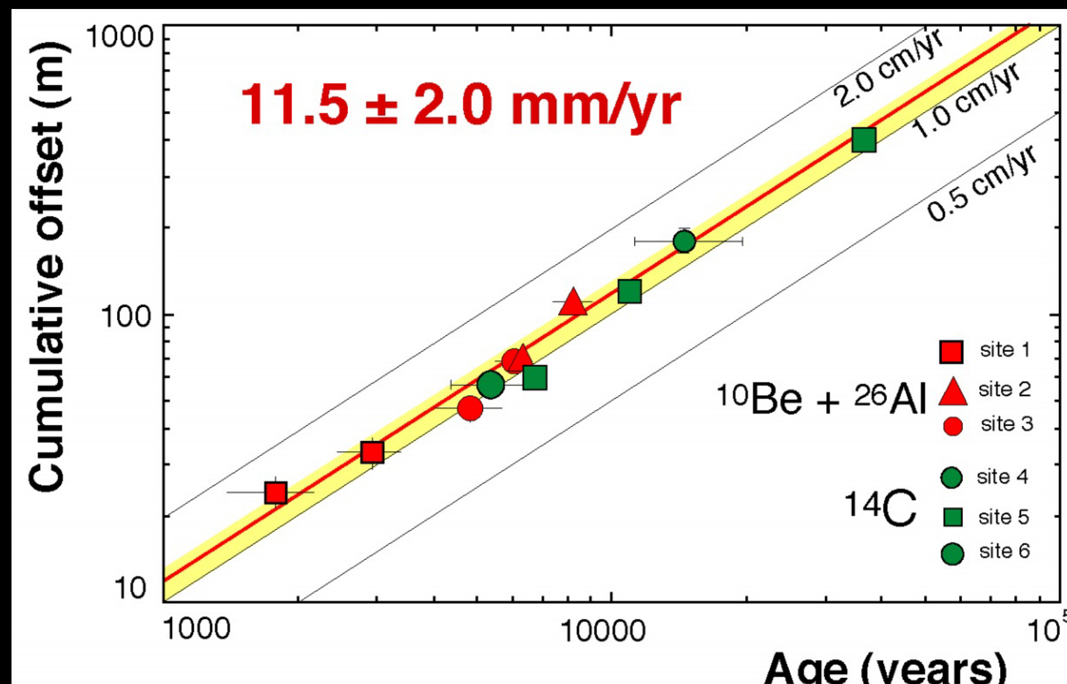

(van der Woerd et al, 2000)

High Resolution Imagery

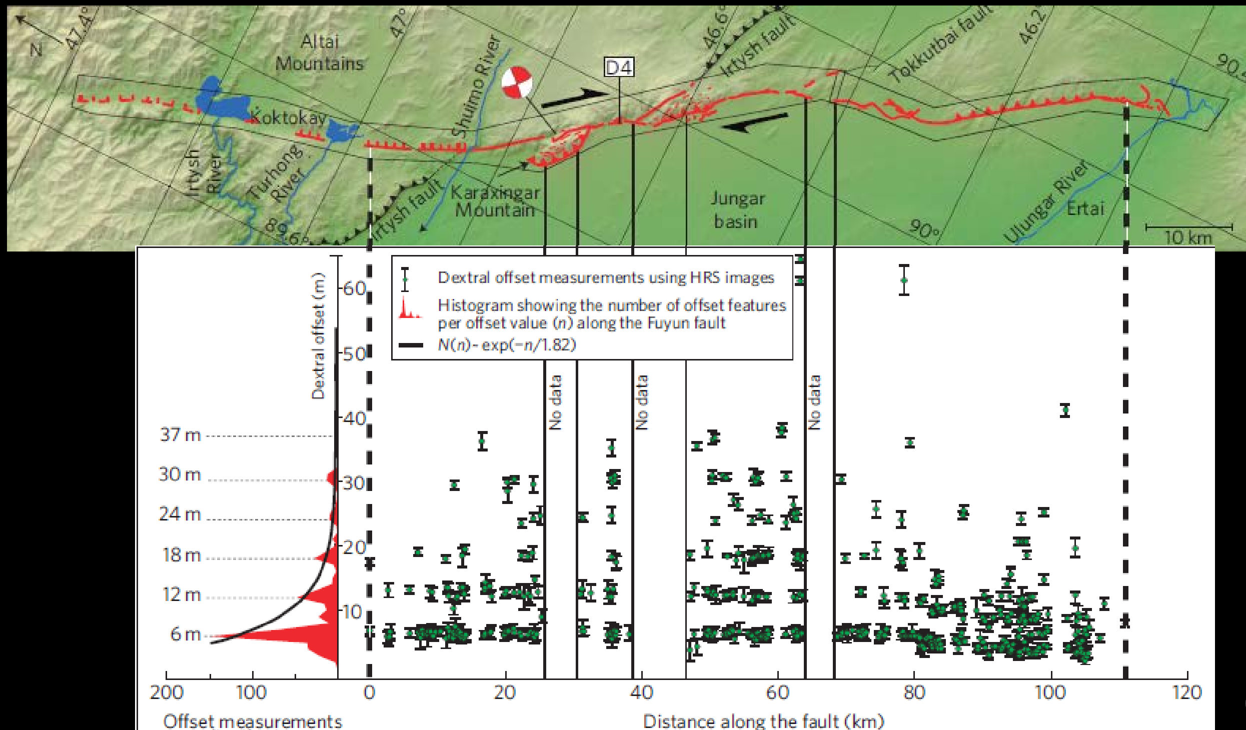

(Klinger et al, 2010)

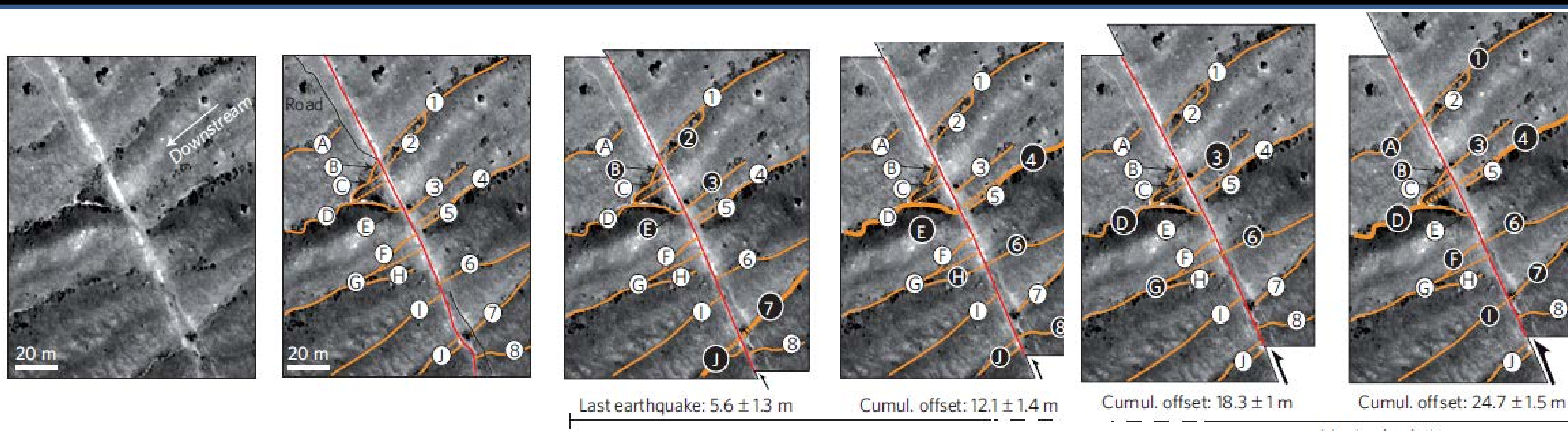

The 3d Dimension

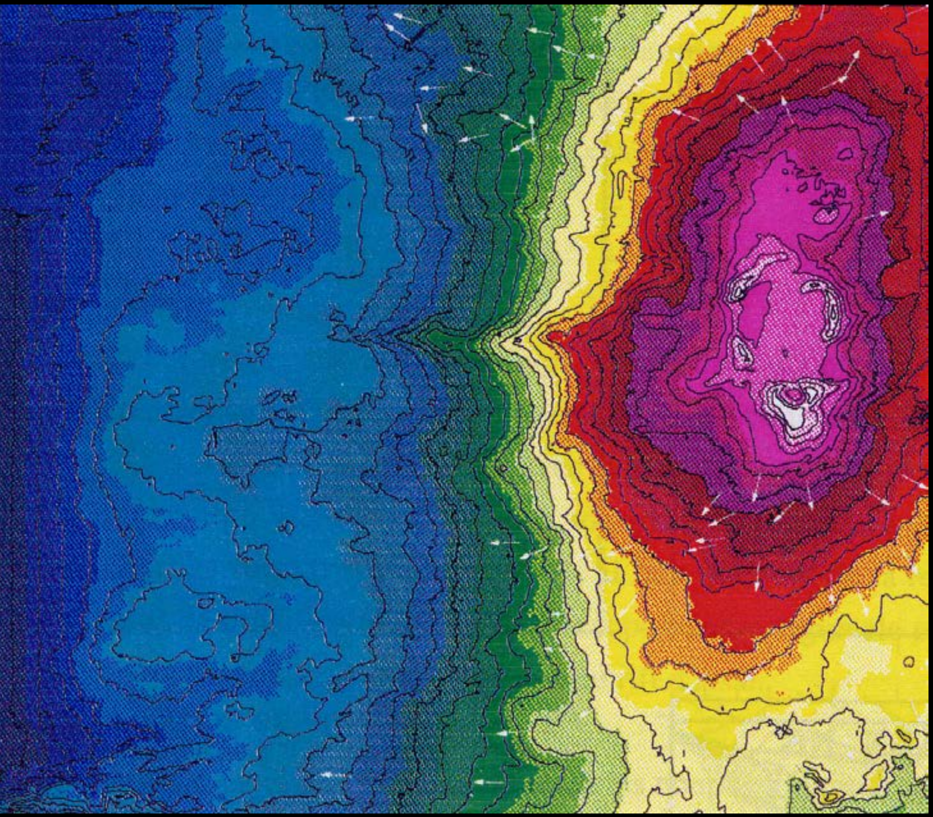

Reconstructed topography after restoration of vertical displacements

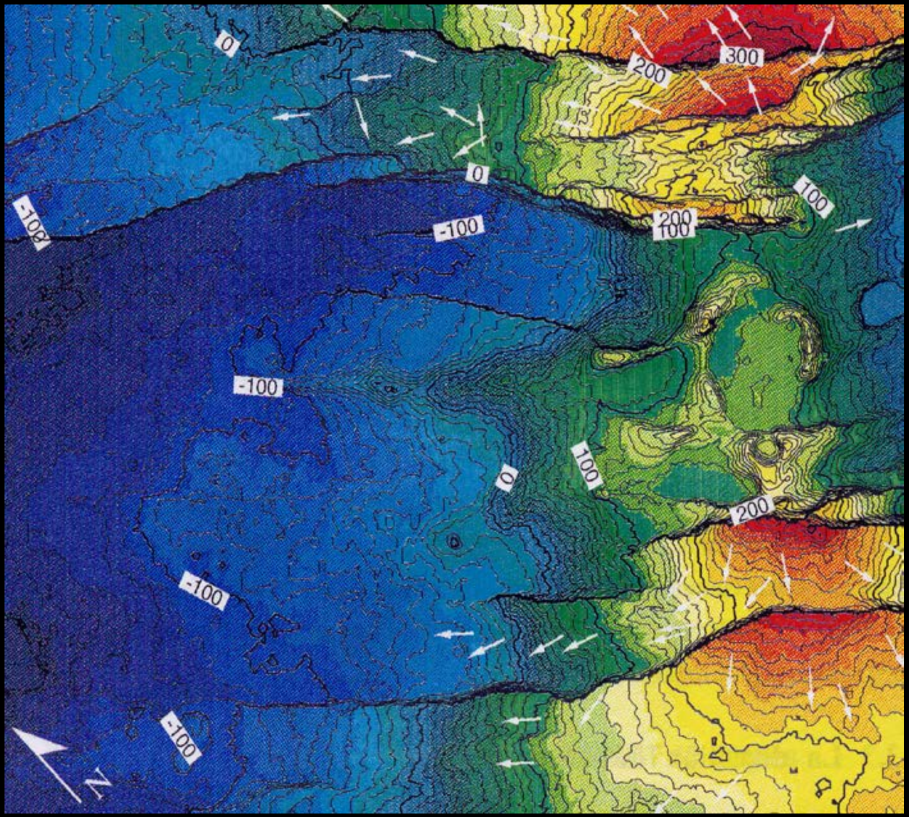

Current topography

(De Chabalier and Avouac, 1995)

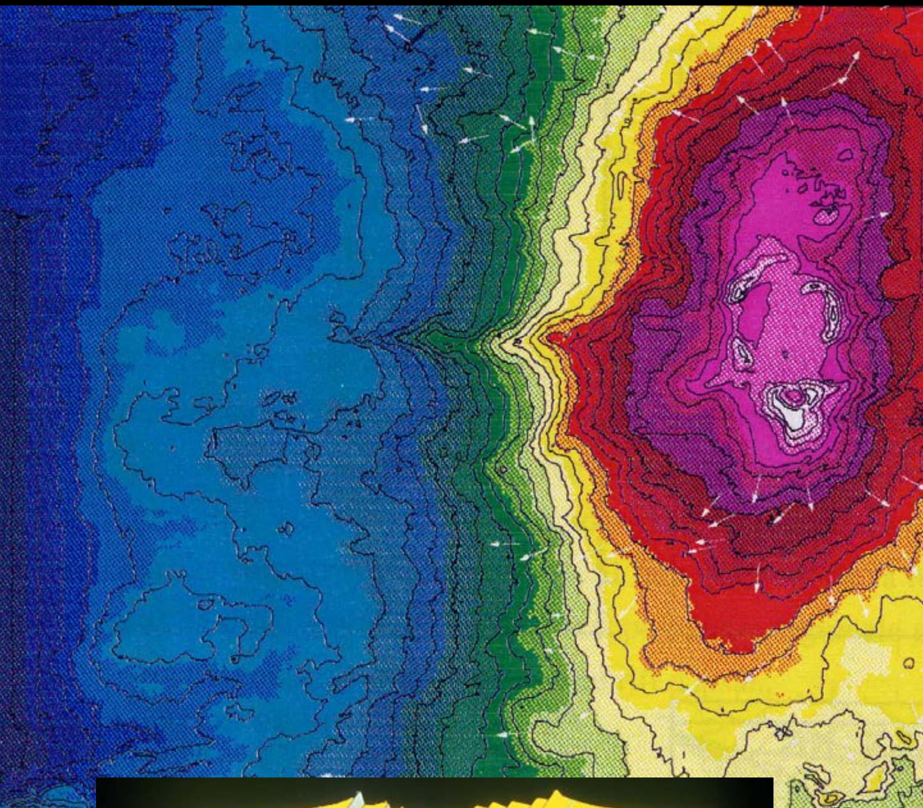

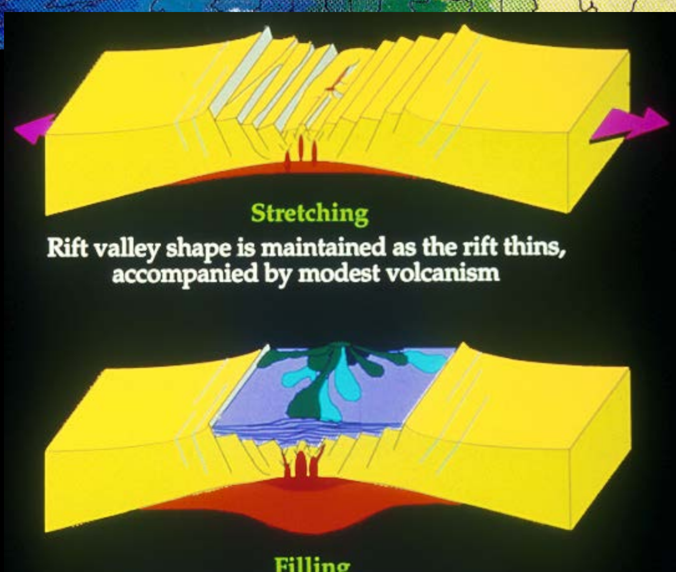

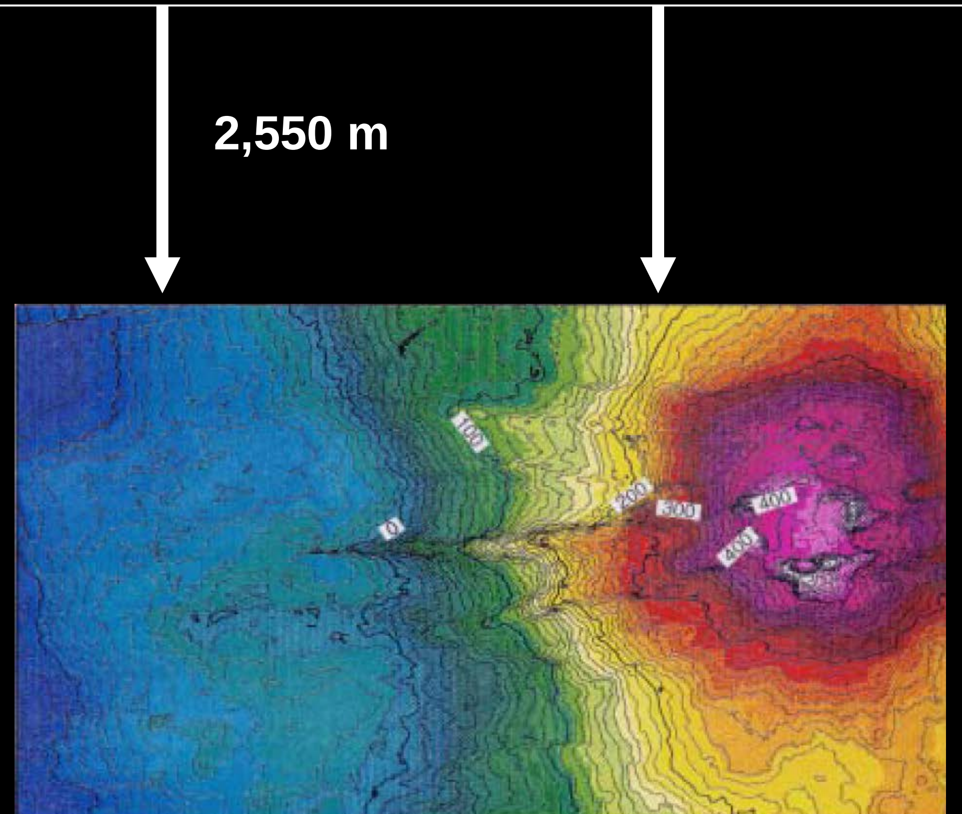

Reconstructed topography after restoration of vertical displacements and horizontal stretching

(De Chabalier and Avouac, 1995)

The 3d Dimension

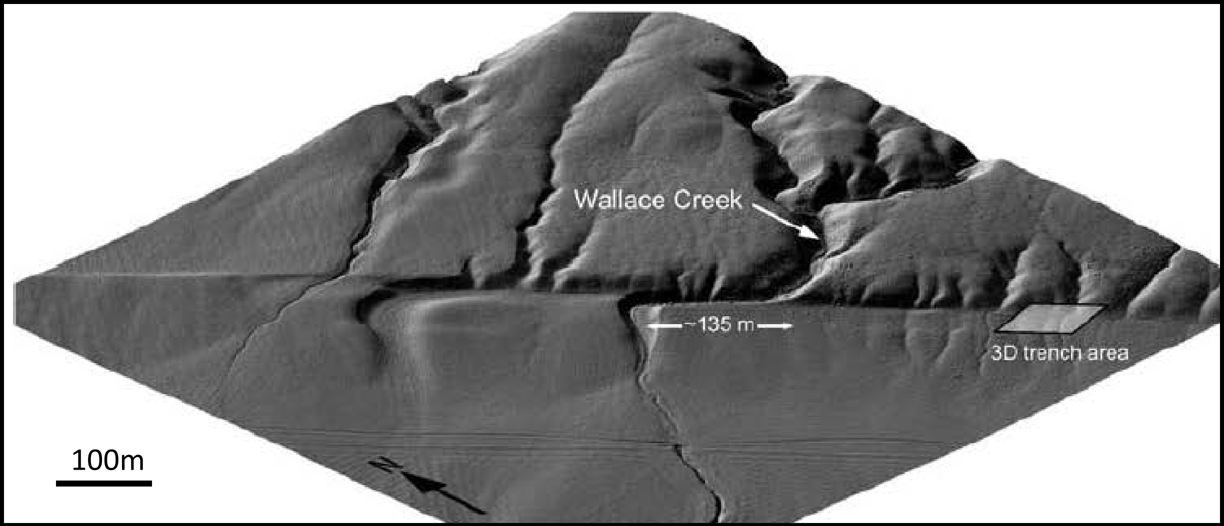

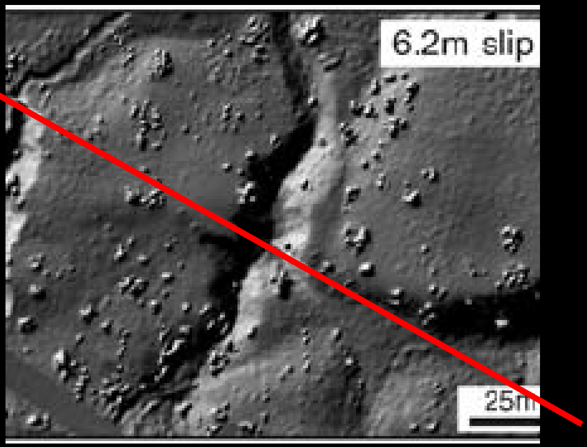

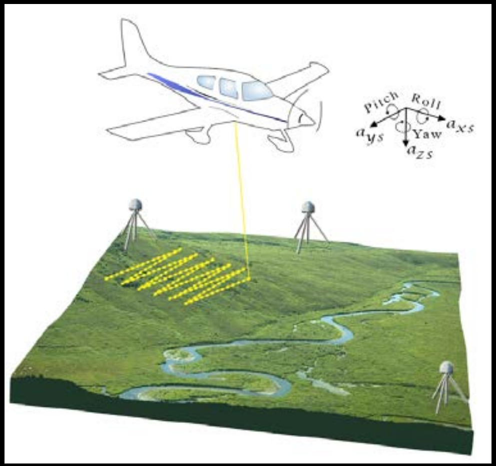

LiDAR, unstripped vegetation,

(Zielke et al, BSSA, 2012)

Image Geodesy
Sub-Pixel Correlation

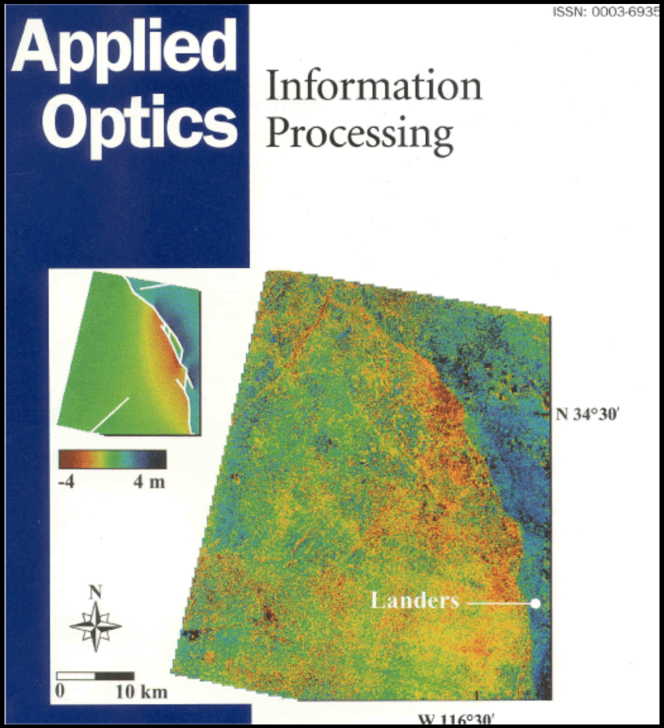

(van Puymbroeck et al, 2000)

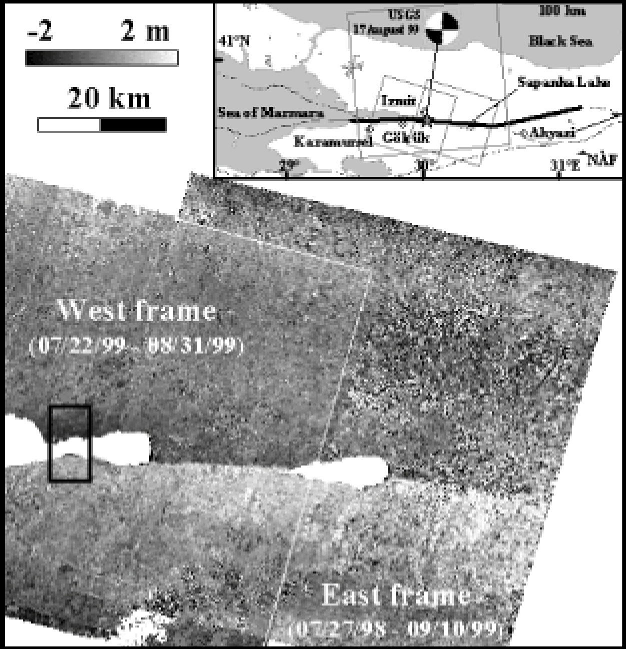

(Michel et al, 2002)

Co-registration of Optically Sensed Images and Correlation

Sébastien Leprince,
Francois Ayoub,
B. Conejo,
Jiao Lin,

❶ **Satellite imagery** acquired at different times, any resolution, possibly by different sensors

❷ **Automatic registration** with accuracy of 1/10 of the pixel size (sub-pixel)

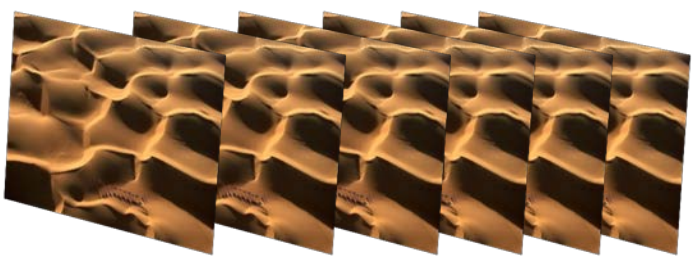

Time

❸ **Automatic comparison** of images to measure motion

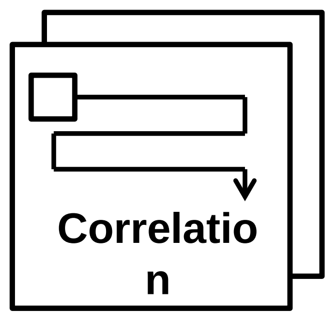

❹ **Ground deformation**

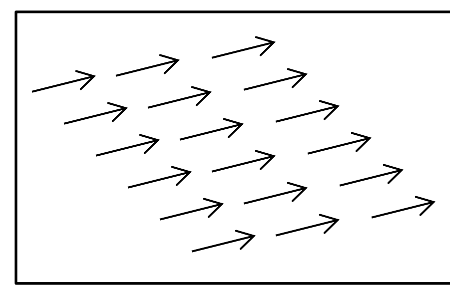

Vector field

(Leprince et al., IEEE TGRS, 2007)

http://www.tectonics.caltech.edu/slip_history/spot_coseis/

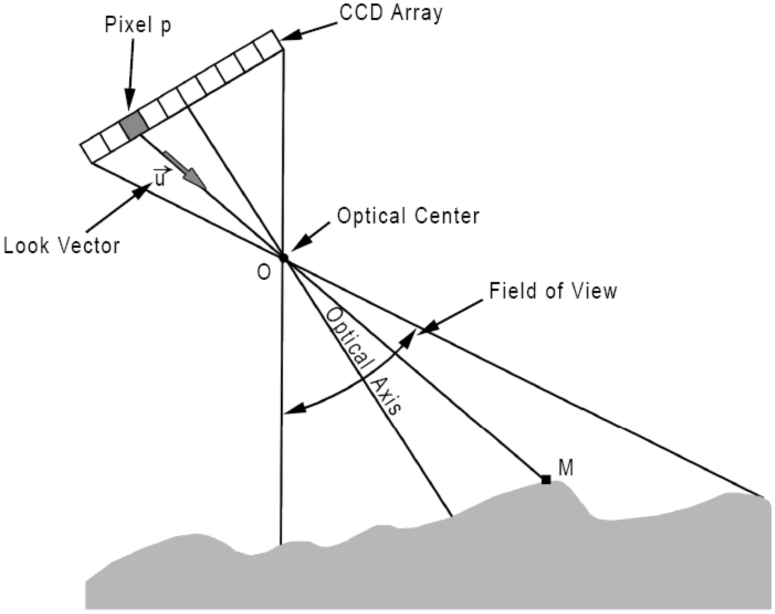
Pixel p
CCD Array
Optical Center
Look Vector
O
Field of View
Optical Axis
M

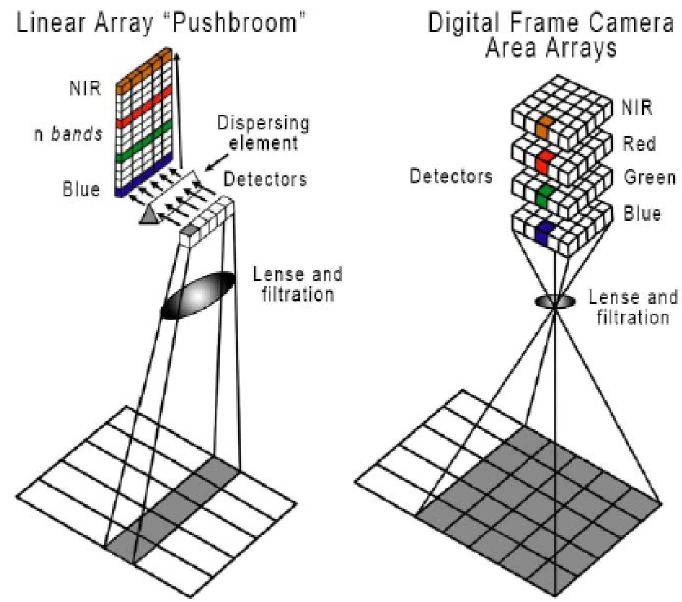
Linear Array "Pushbroom"
NIR
n bands
Blue
Dispersing element
Detectors
Lense and filtration
Digital Frame Camera
Area Arrays
Detectors
NIR
Red
Green
Blue
Lense and filtration

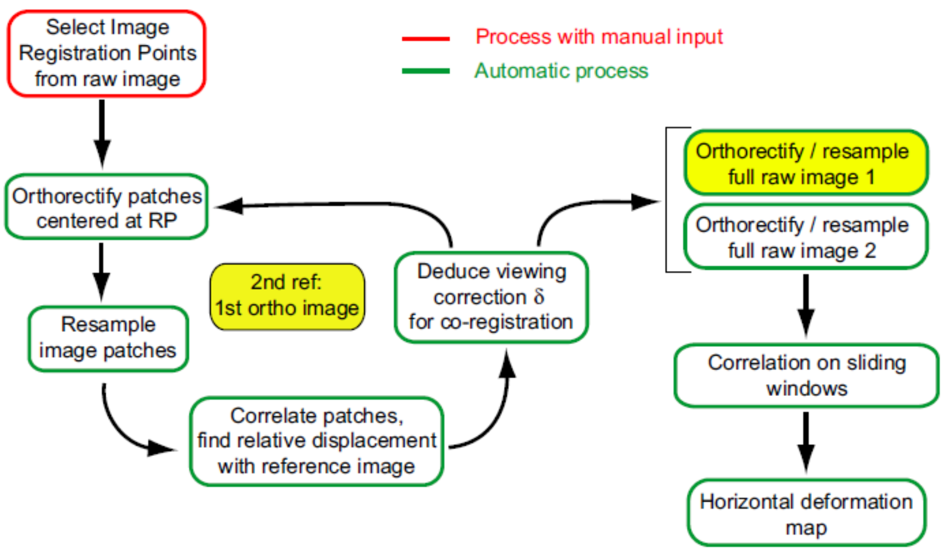
Select Image Registration Points from raw image
Process with manual input
Automatic process
Orthorectify patches centered at RP
2nd ref: 1st ortho image
Resample image patches
Deduce viewing correction δ for co-registration
Correlate patches, find relative displacement with reference image
Orthorectify / resample full raw image 1
Orthorectify / resample full raw image 2
Correlation on sliding windows
Horizontal deformation map

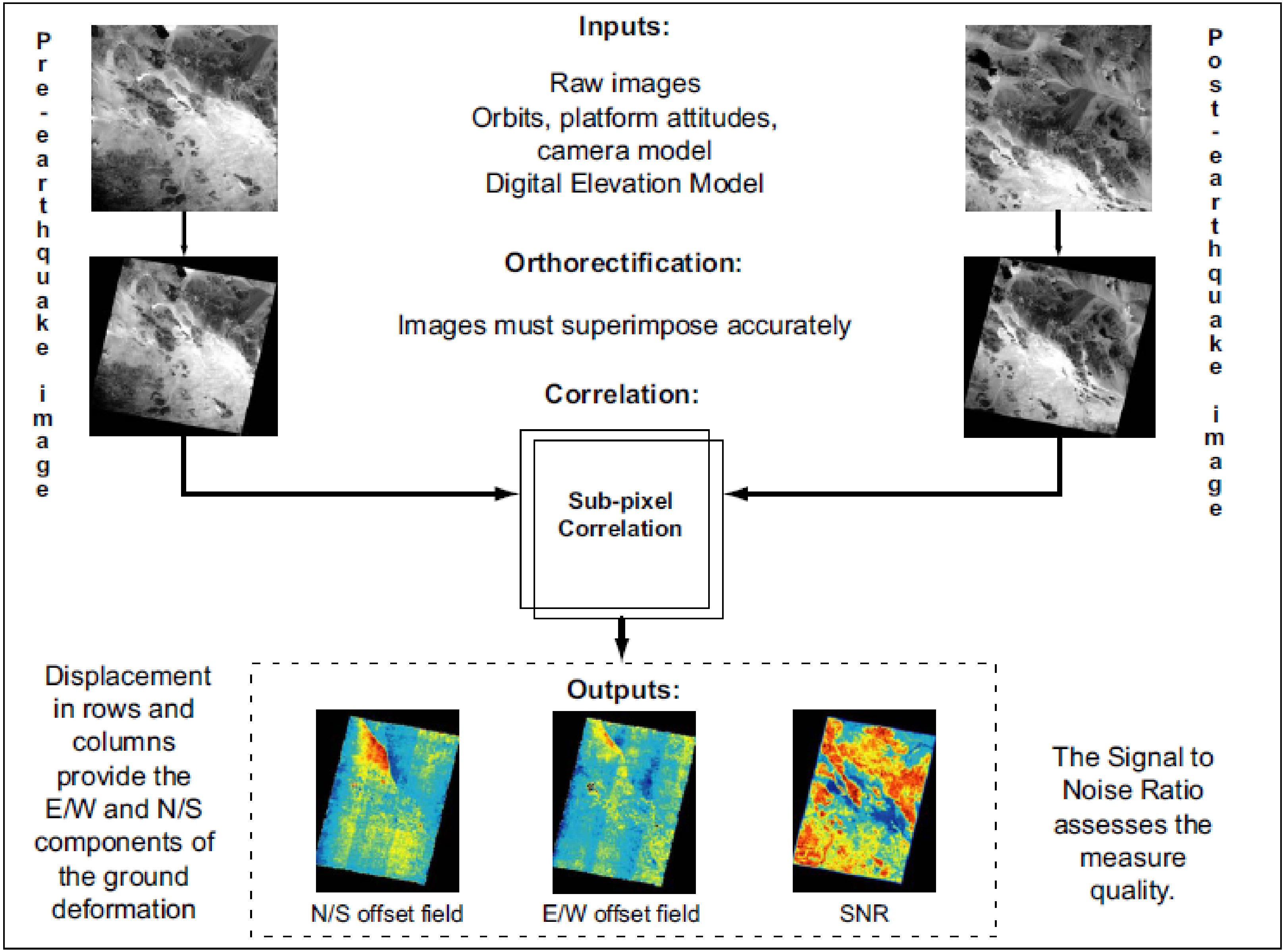

(Leprince et al, 2007)

Solving for 3-D displacements and the topography with 4 images.

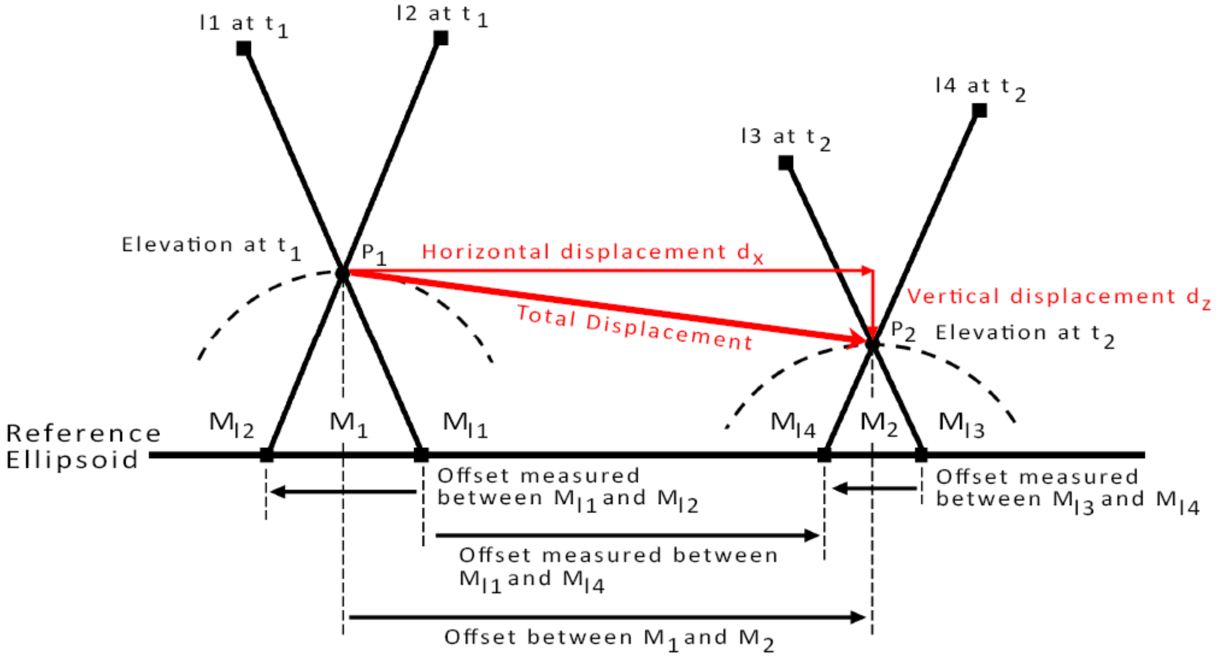

The Mw7.1 Hectore Mine Earthquake

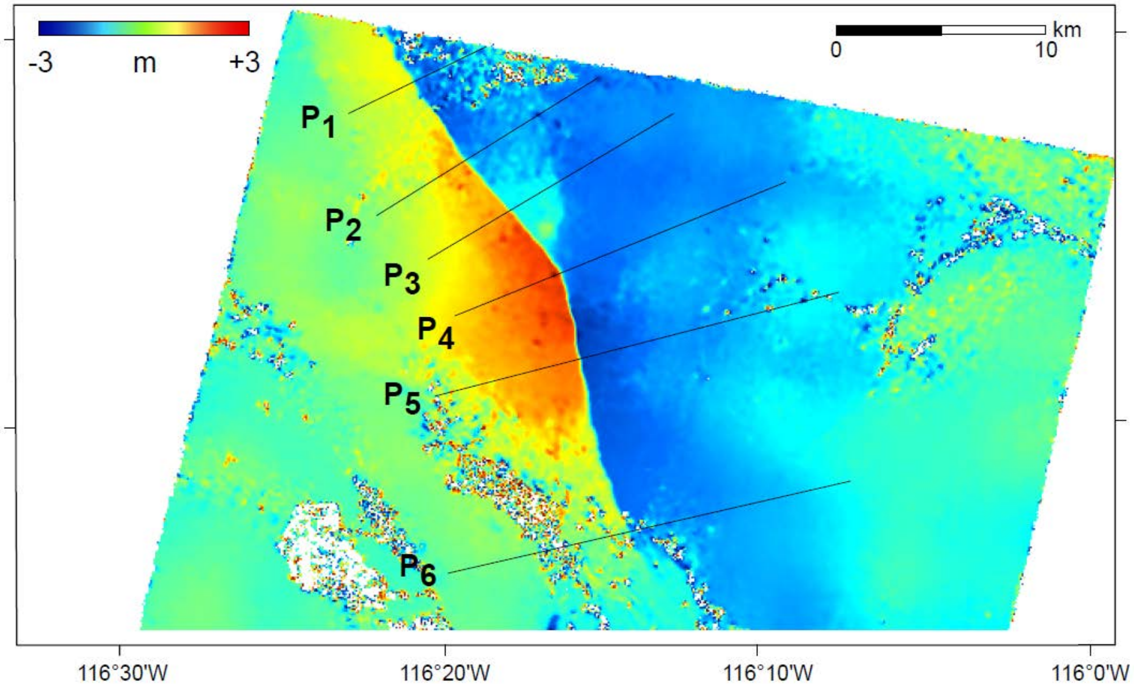

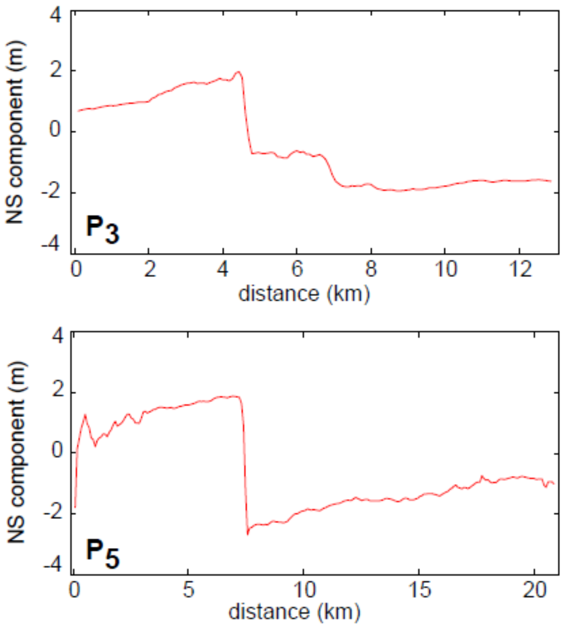

(Sebastien Leprince)

The 2010, Cucapah El-Mayor EQ

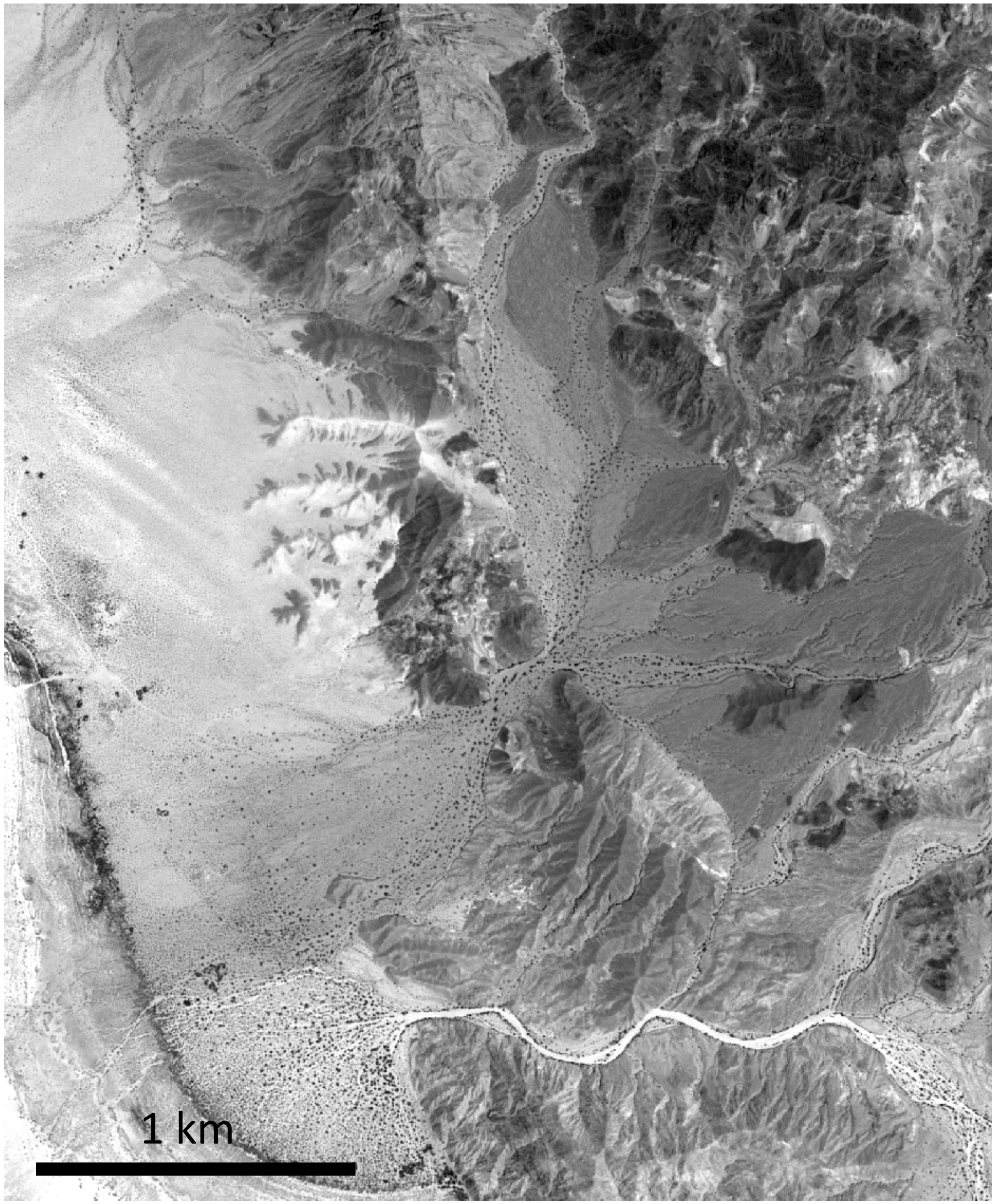

Pre-earthquake images:

- Quickbird **09/21/2006**,
  Along-track angle -1.23°
  Across-track angle -9.8°

- Worldview **09/16/2008**,
  Along-track angle -10.8°
  Across-track angle 13.5°

Post-earthquake images:

- Worldview **04/10/2011**,
  Along-track angle -13.8 °
  Across-track angle -22.5°

- Worldview **05/19/2011**,
  Along-track angle 14.1°
  Across-track angle 21.6°

(Sebastien Leprince)

The 2010, Cucapah El-Mayor EQ

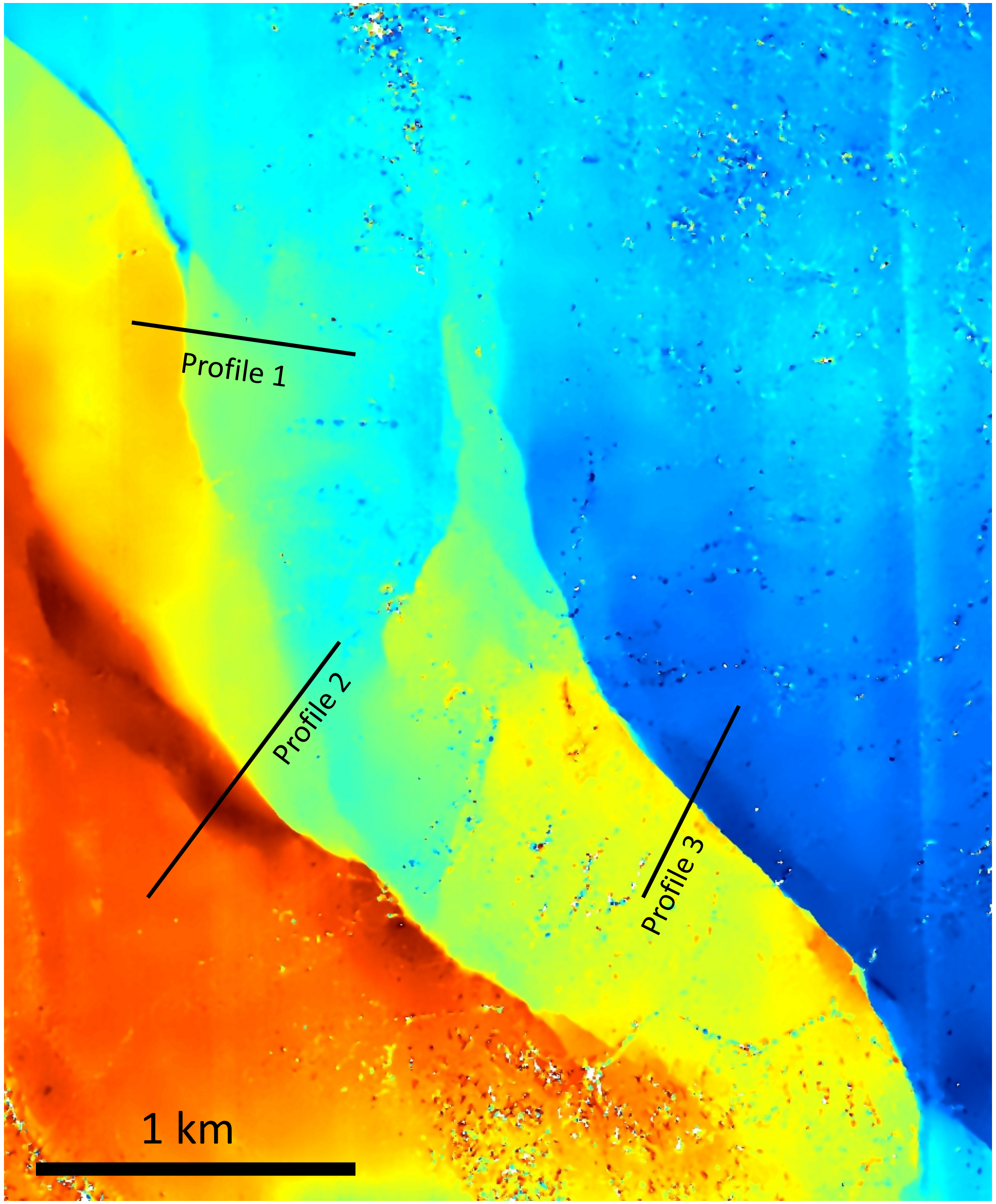

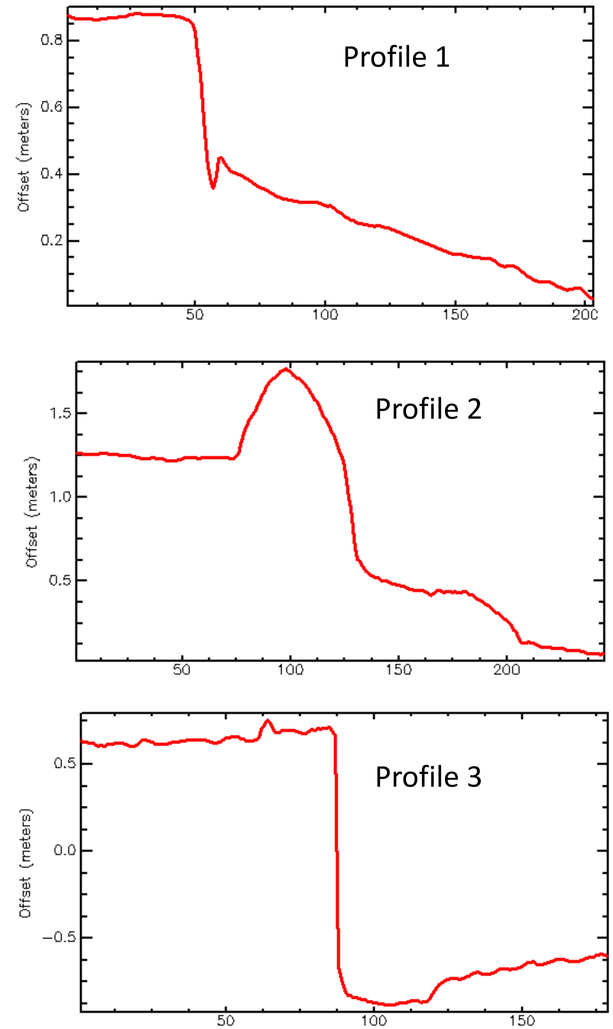

Measurement accuracy better than 10 cm
(Sebastien Leprince)

The 2010, Cucapah El-Mayor EQ

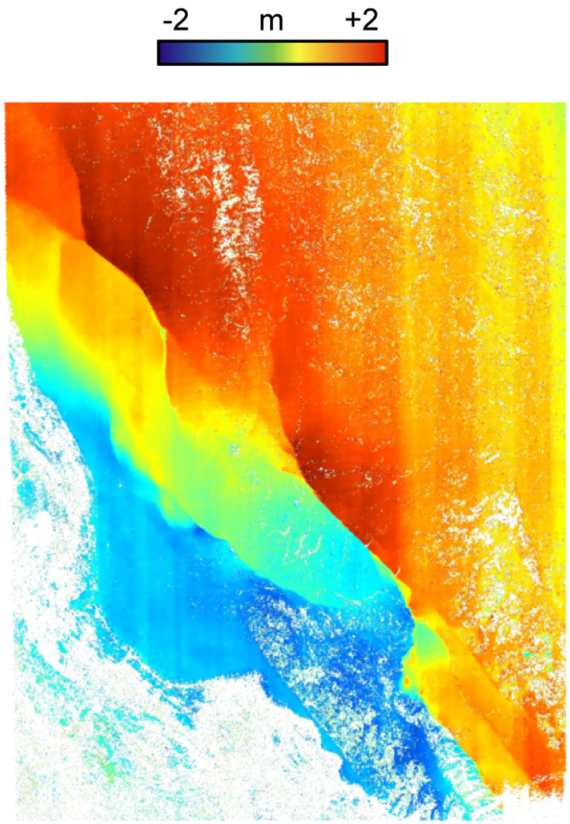

Eastward ground motion

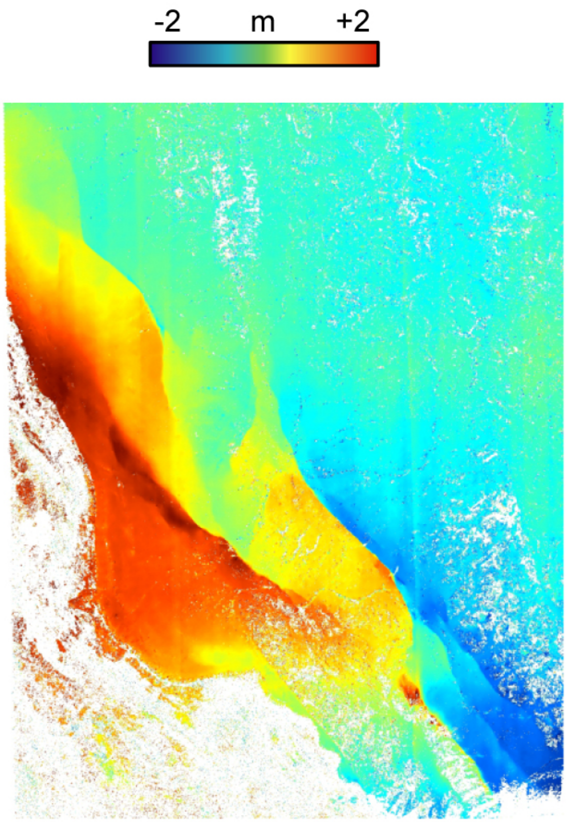

Northward ground motion

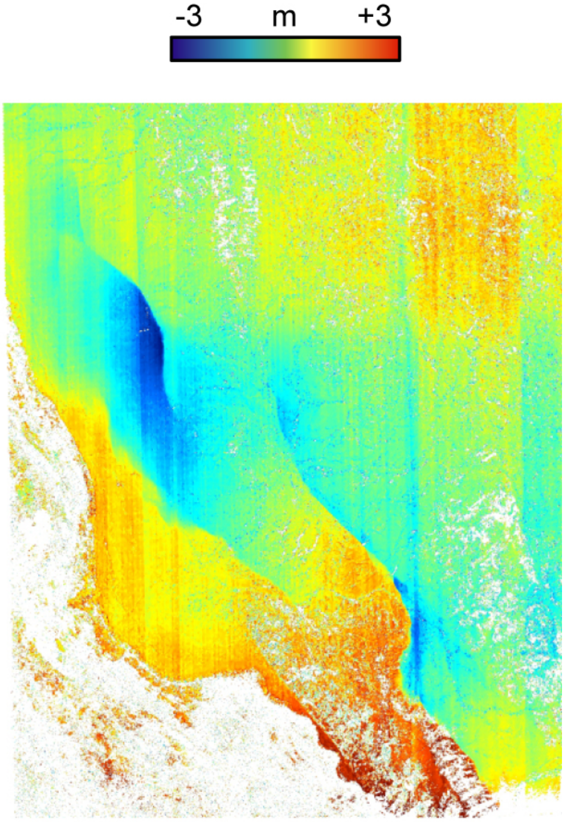

Vertical ground motion

(Sebastien Leprince)

The Sept, 24, 2013, Mw7.7 Balochistan Earthquake

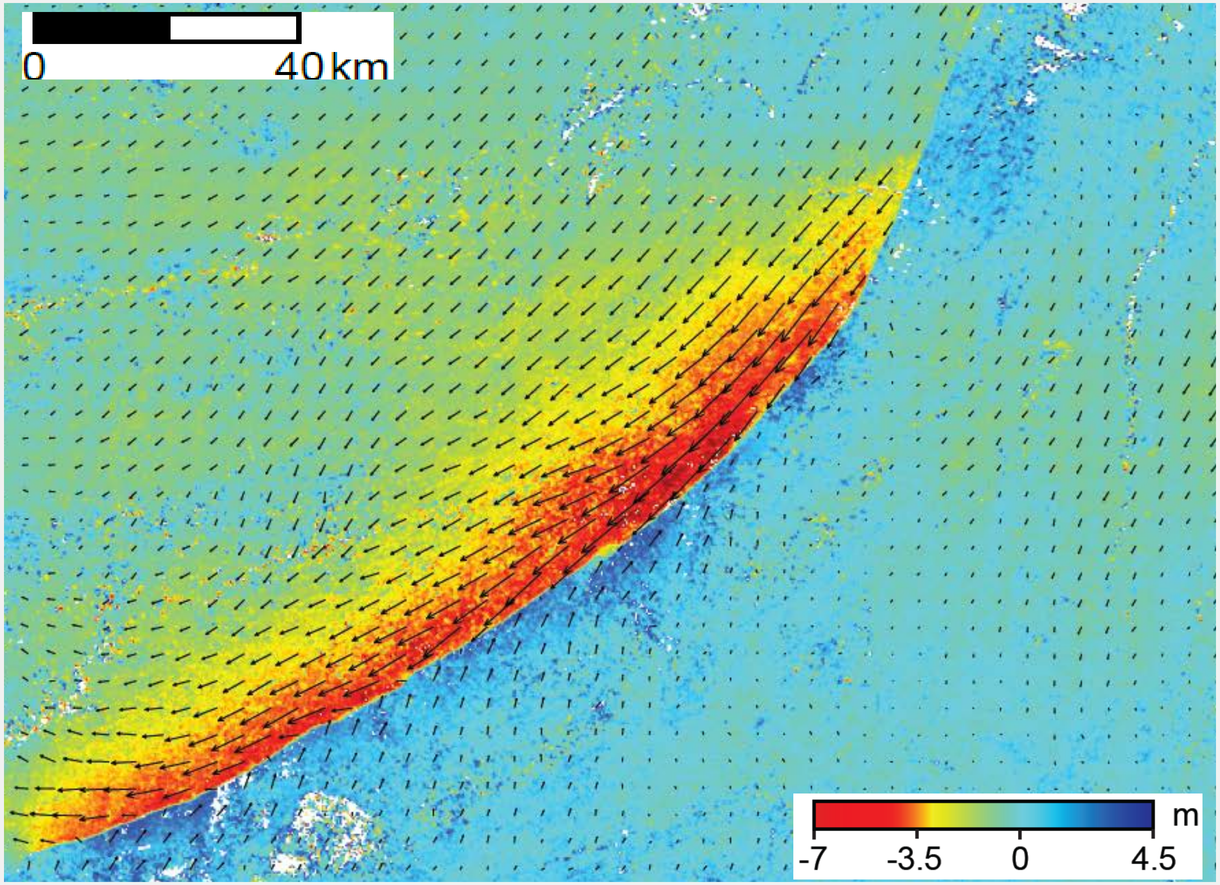

Surface displacements measured from correlating 2 Landsat-8 images

(Francois Ayoub)

The Sept, 24, 2013, Mw7.7 Balochistan Earthquake

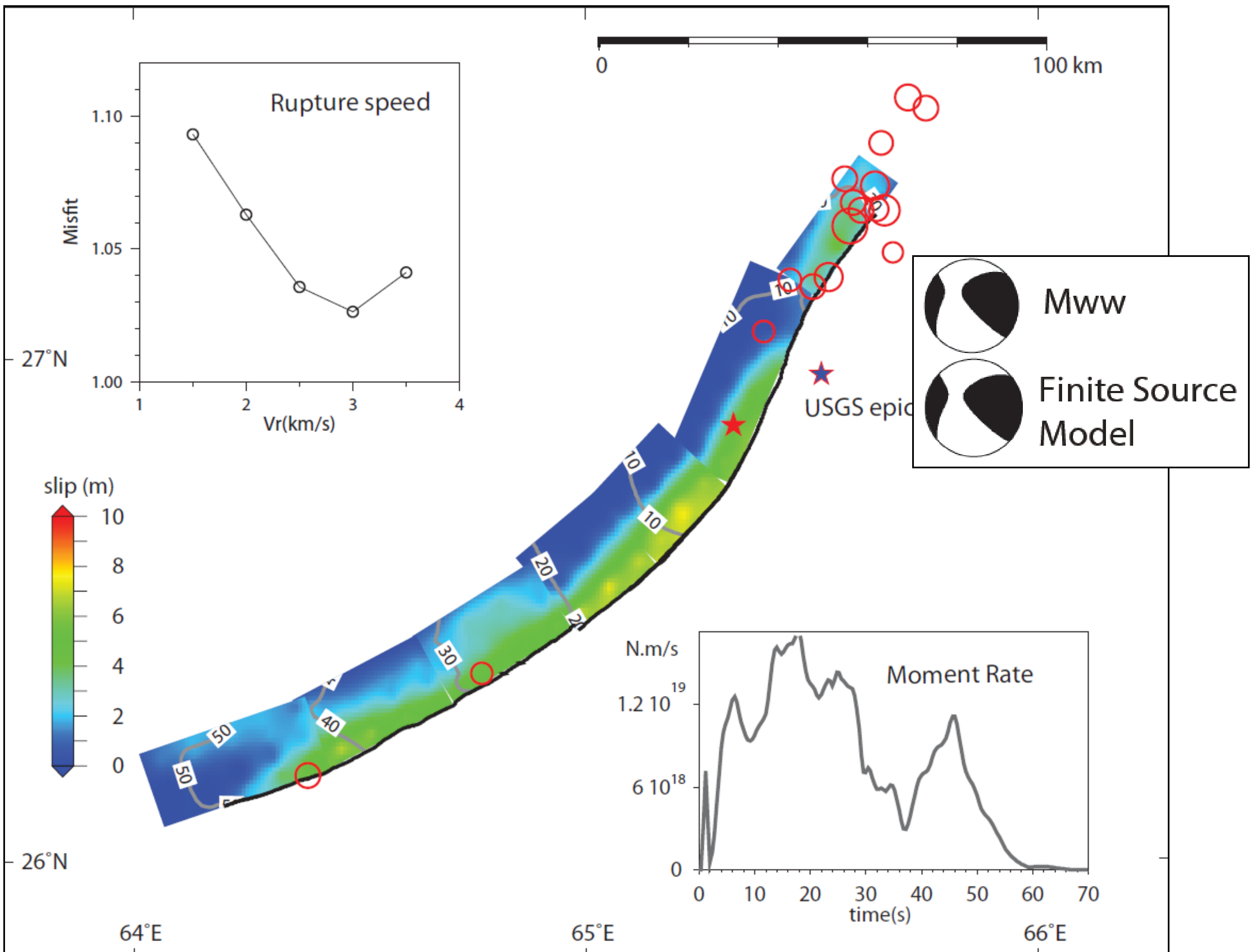

The Krafla volcanic crisis

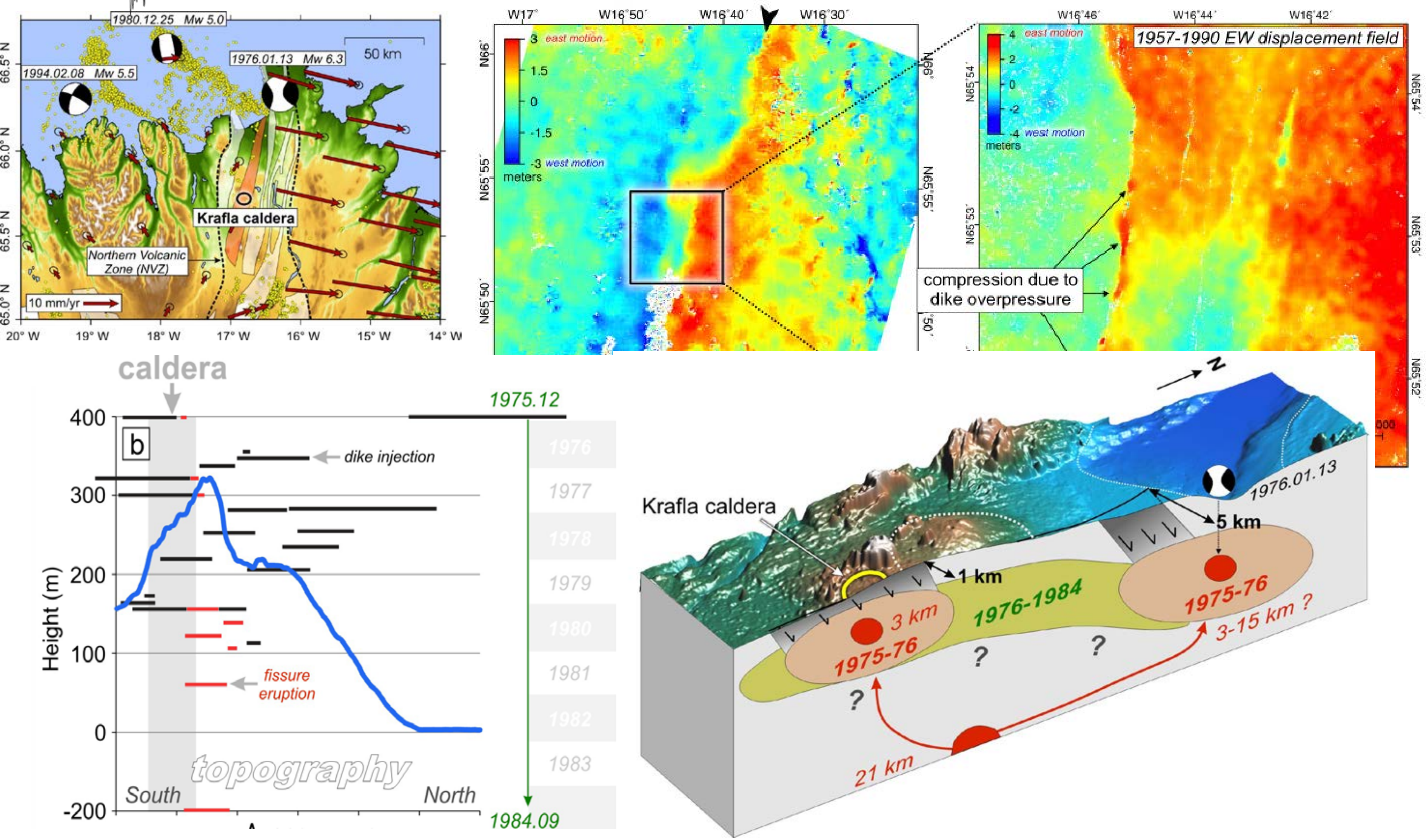

(Hollingsworth et al, JGR, 2012,2013)

Glacier Monitoring

Multi-temporal Stereo Acquisitions using Worldview GSD 50 cm:

- ***January 30, 2013*** *(x2)*
- ***February 9, 2013*** *(x2)*
- ***February 28, 2013*** *(x2)*

- Bundle adjustment between all images,
- Multi-scale image matching due to large disparities (up to 1000 pixels),
- Regularized matching because of occlusions

Franz Josef Glacier

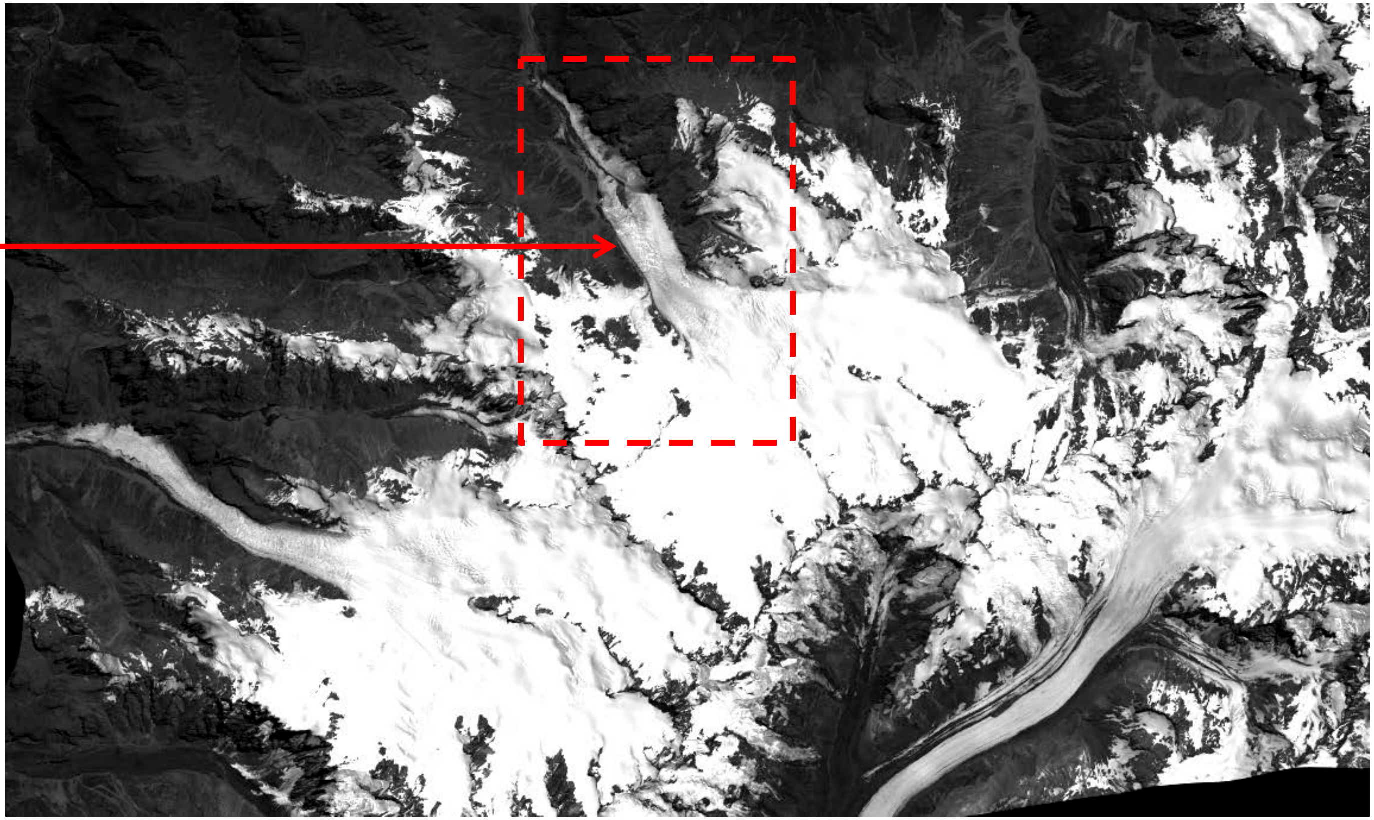

2 km

(Sebastien Leprince)

Glacier Monitoring

- 3D surface displacements -
January 30 and February 9, 2013

2 km

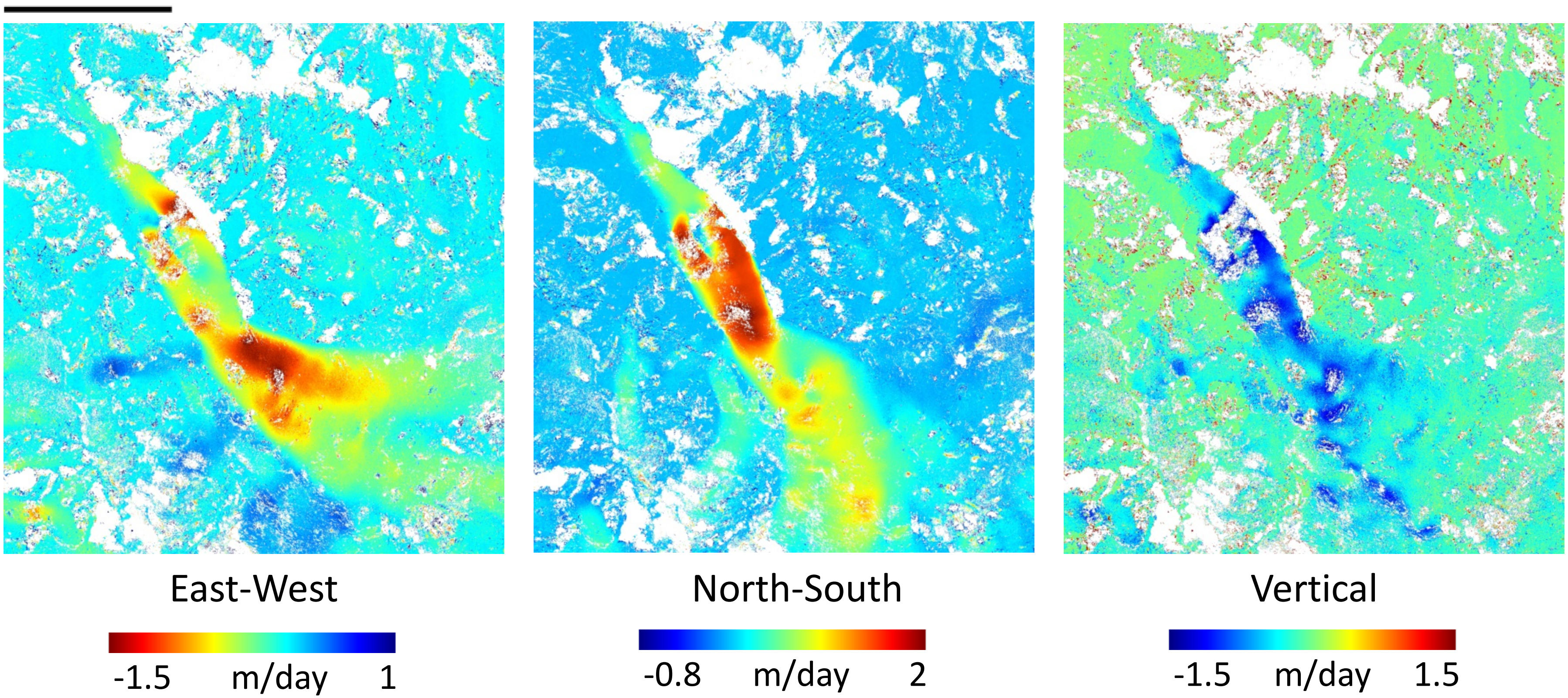

(Sebastien Leprince)

Earthquake Damages from repeated LiDAR survey

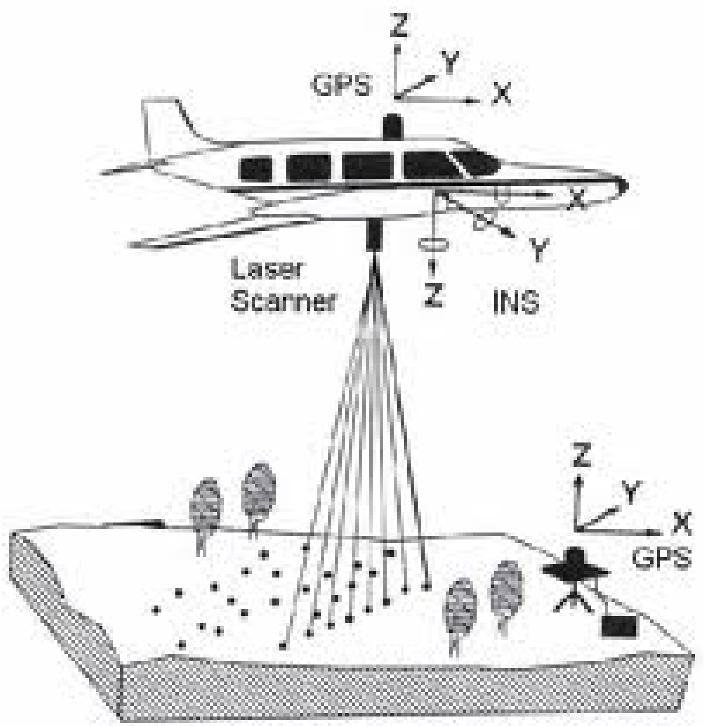

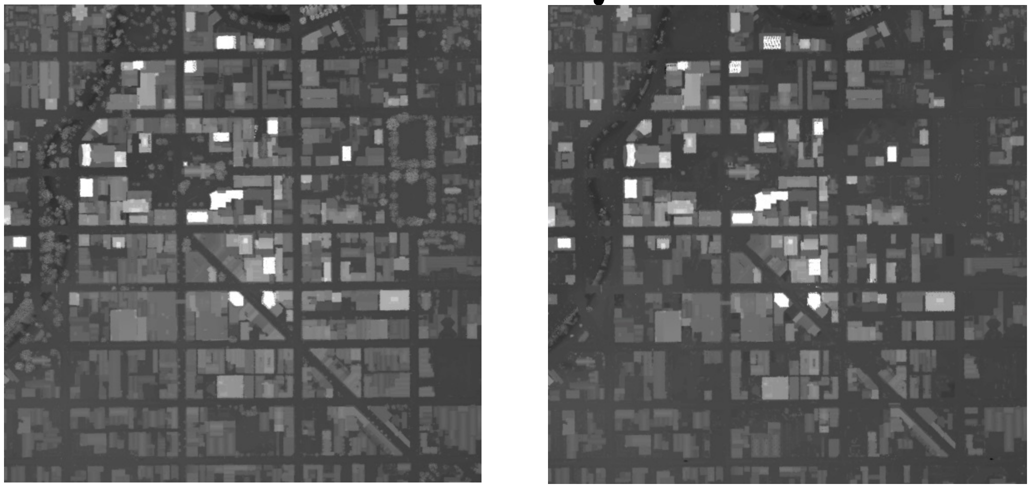

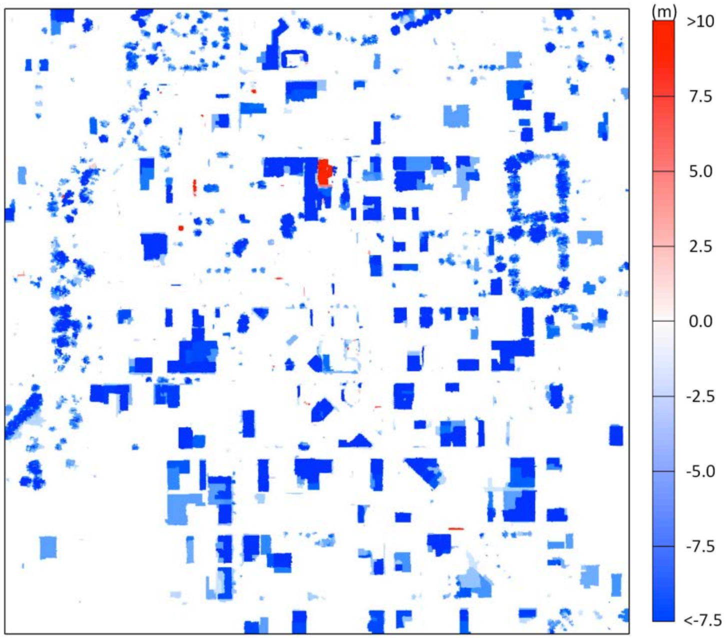

(Bruno Conejo, Sebastien Leprince)

Dunes Dynamics

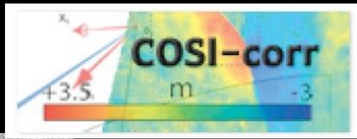

Nili Patera - HiRISE

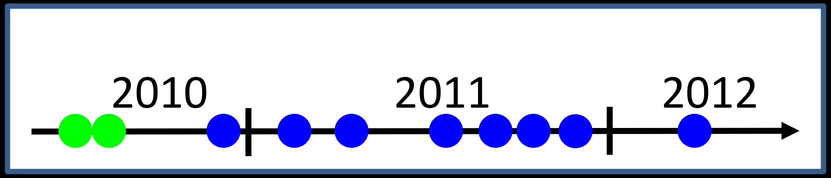

Time-series of 9 HiRISE images covering one Mars year

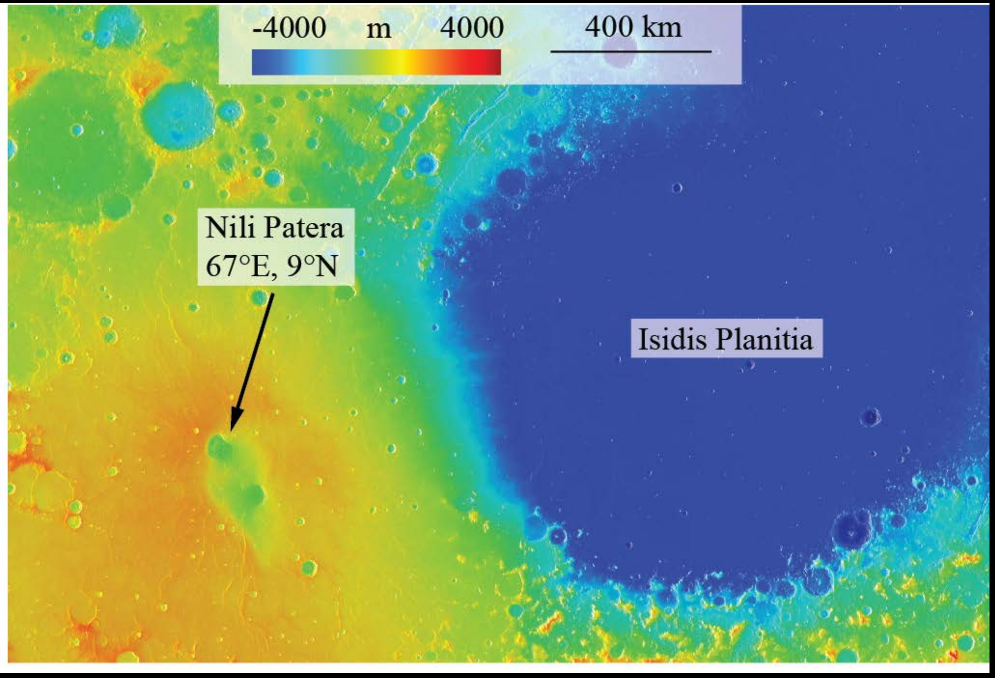

(Bridges et al, 2012; Ayoub et al, in press,)

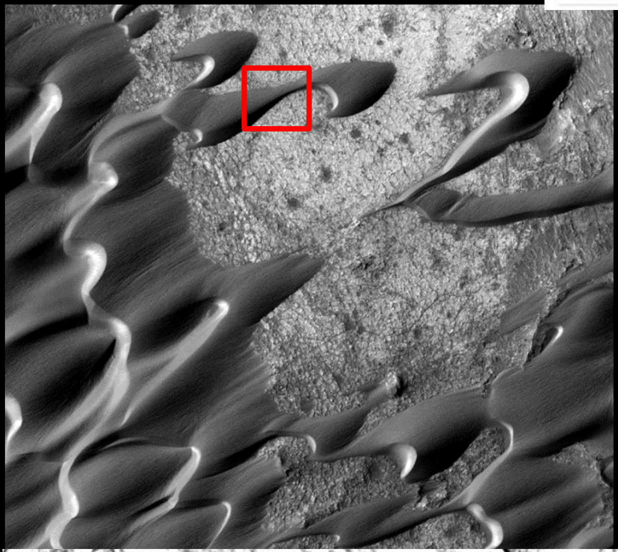

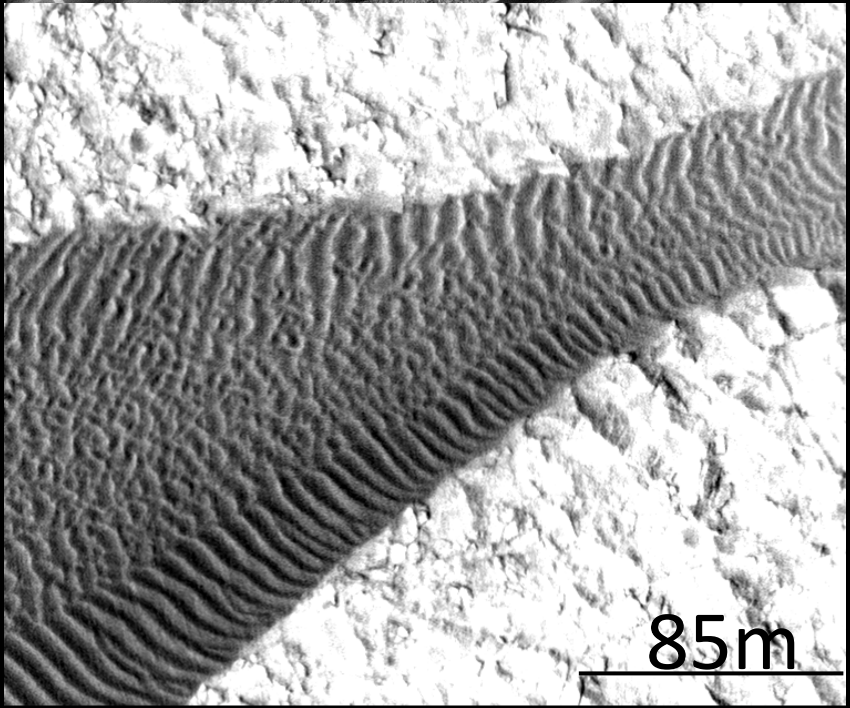

(Francois Ayoub)

Dunes Dynamics

Measurement of ripple migration

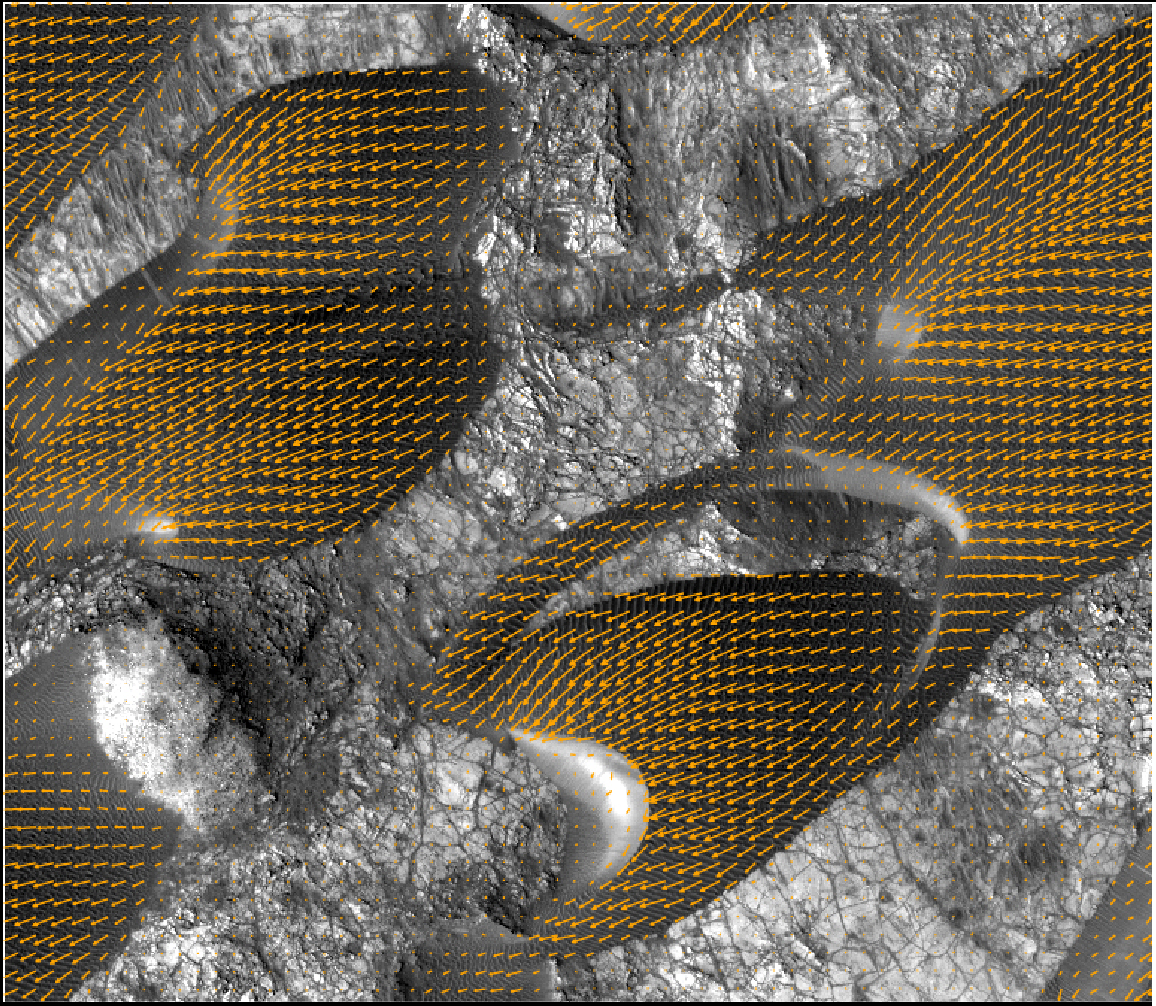

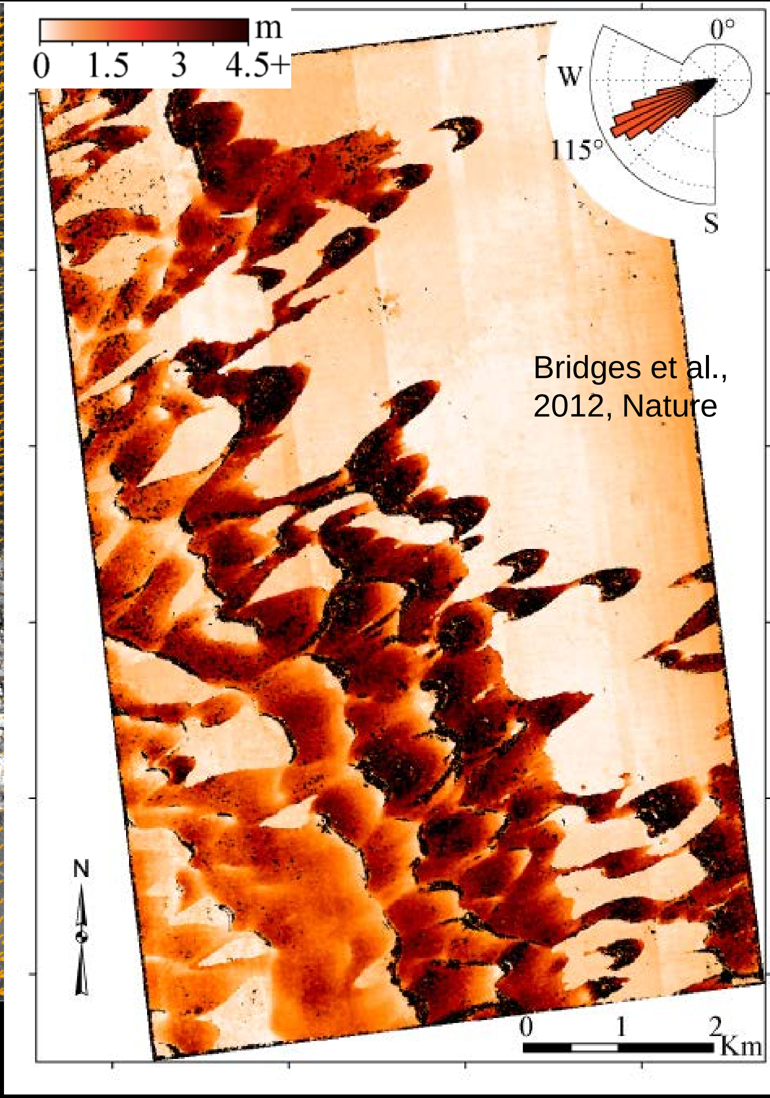

(Francois Ayoub)

Dunes Dynamics

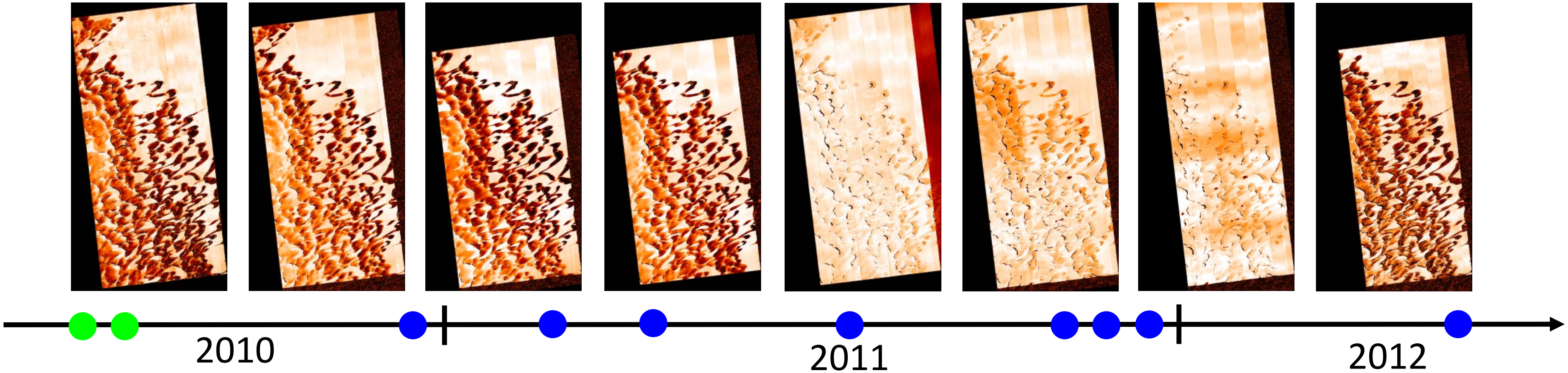

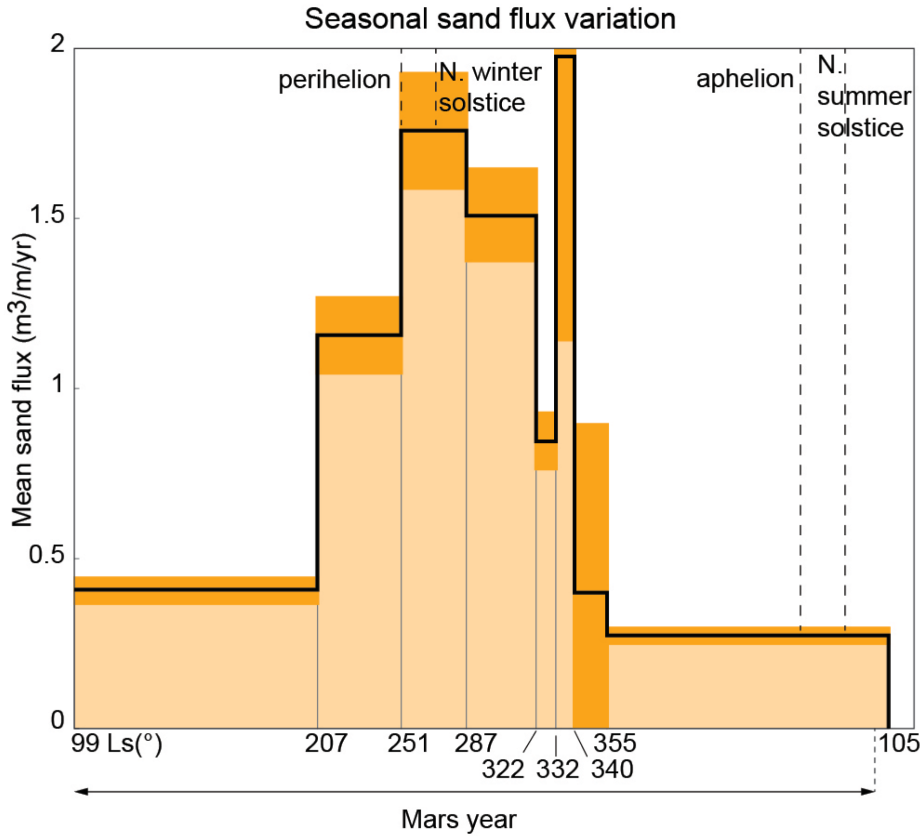

Sand flux variations estimated from ripple migration

(Francois Ayoub)

Landslides

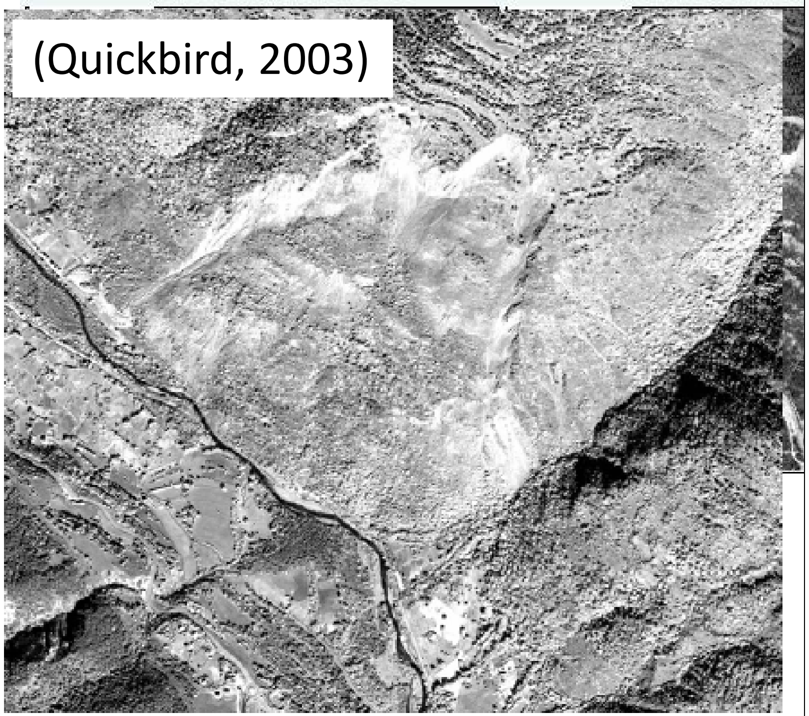

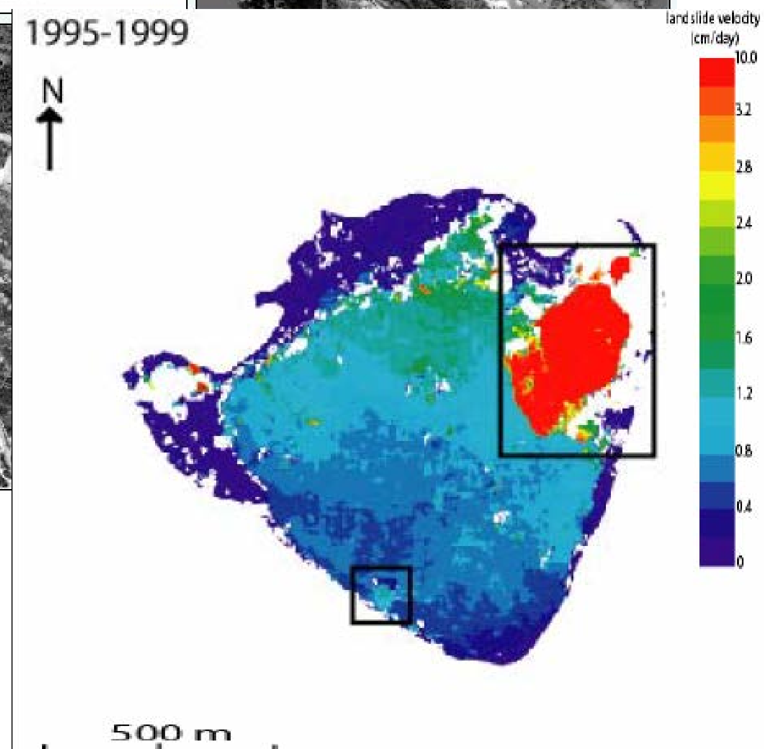

(Delacourt et al, 2004)

Landslides

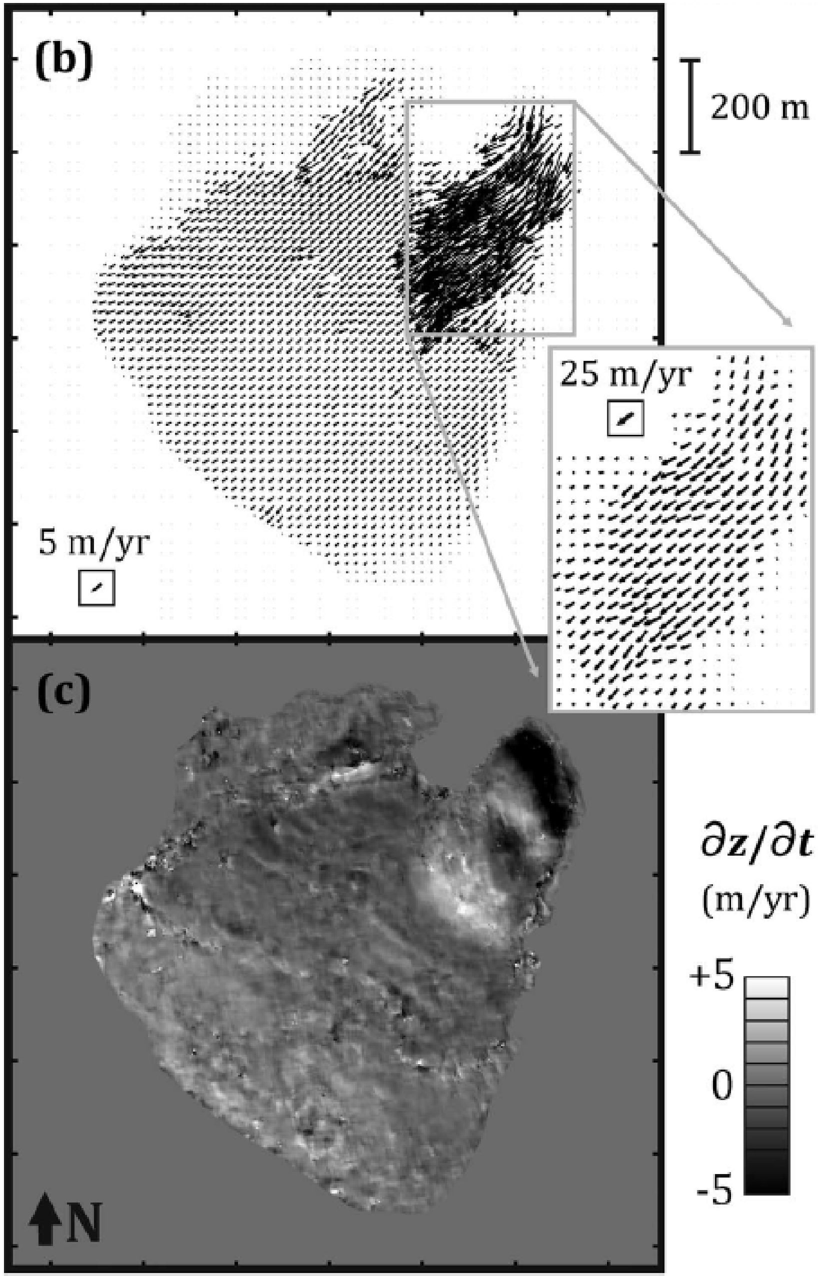

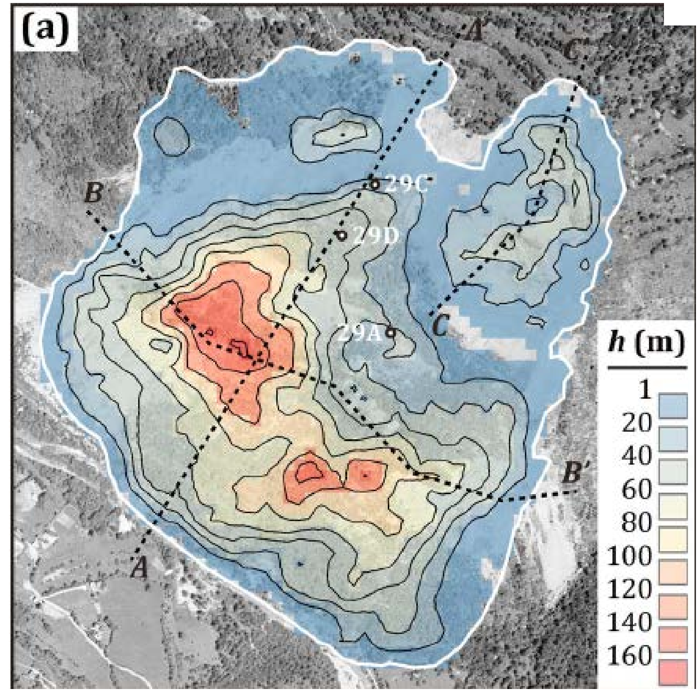

$$\frac{\partial z}{\partial t} = -\nabla \cdot (f \boldsymbol{u}_{\mathrm{surf}} h)$$

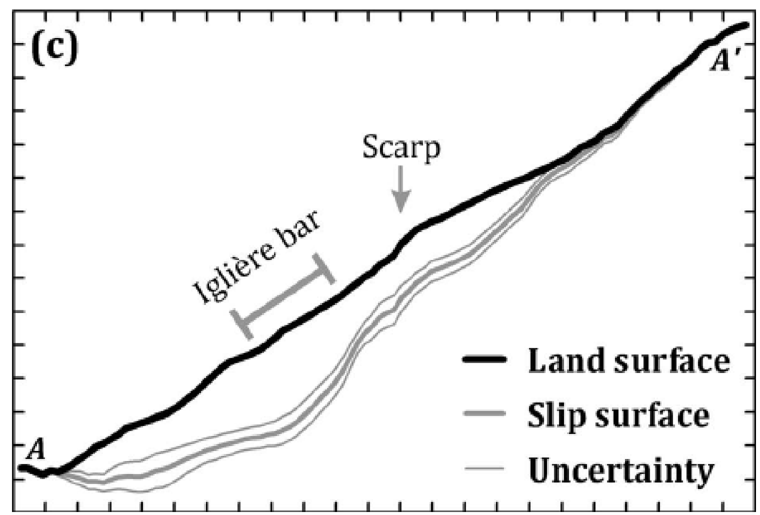

(Booth et al., 2013)

Next: Staring imaging

Some science themes which might then be addressed:

- Earthquakes: details of seismic ruptures
- Volcanoes: details of eruptions
- Glacier: volume budget, episodic flow
- Landslides: episodic flow, volume estimate

Geo Seismic Imager

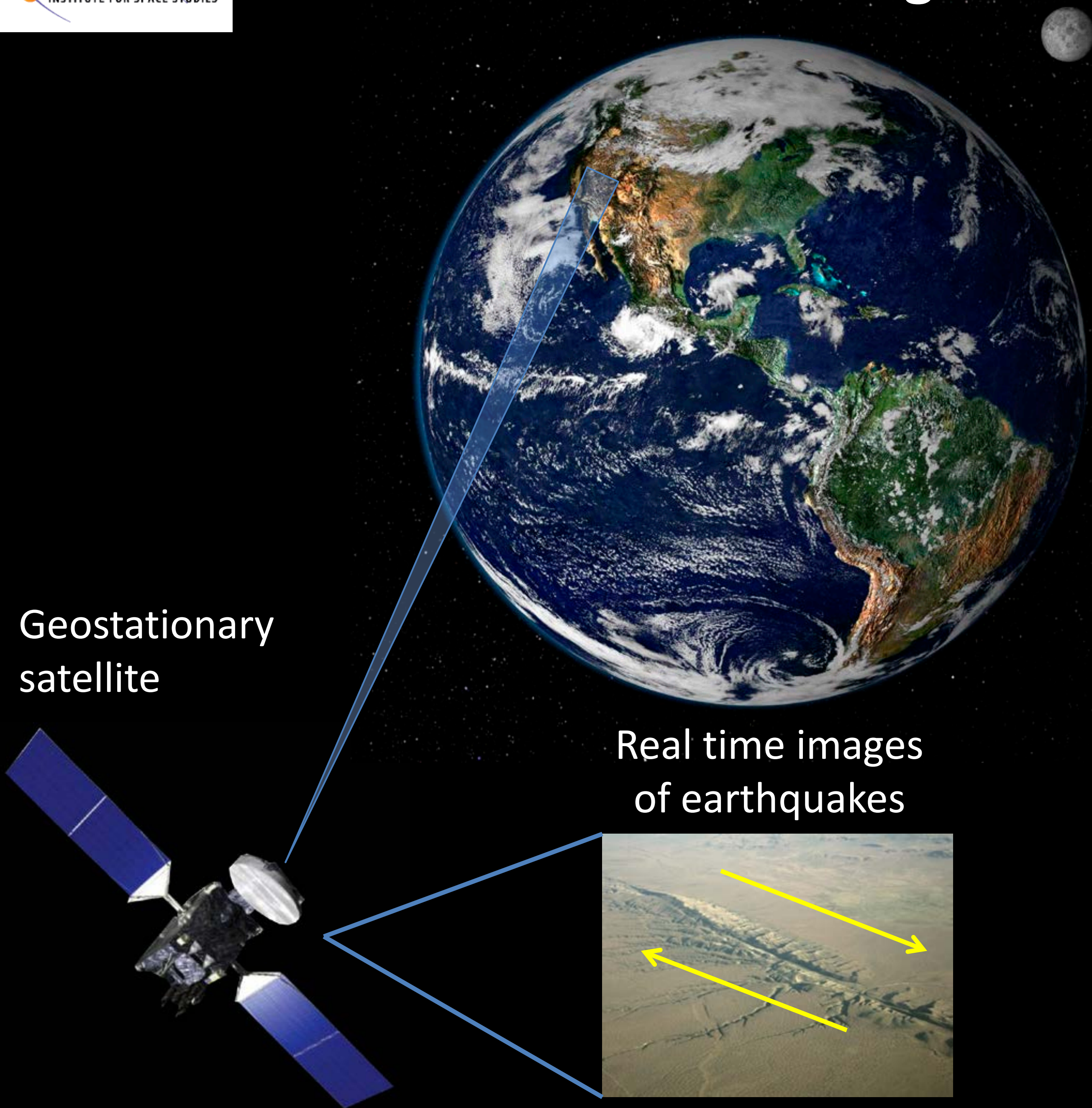

Remi Michel
Dave Redding
Erkin Sidick
Pablo Ampuero
Sebastien Leprince

A M_w 7.0 quake seen by a 4 m GSI

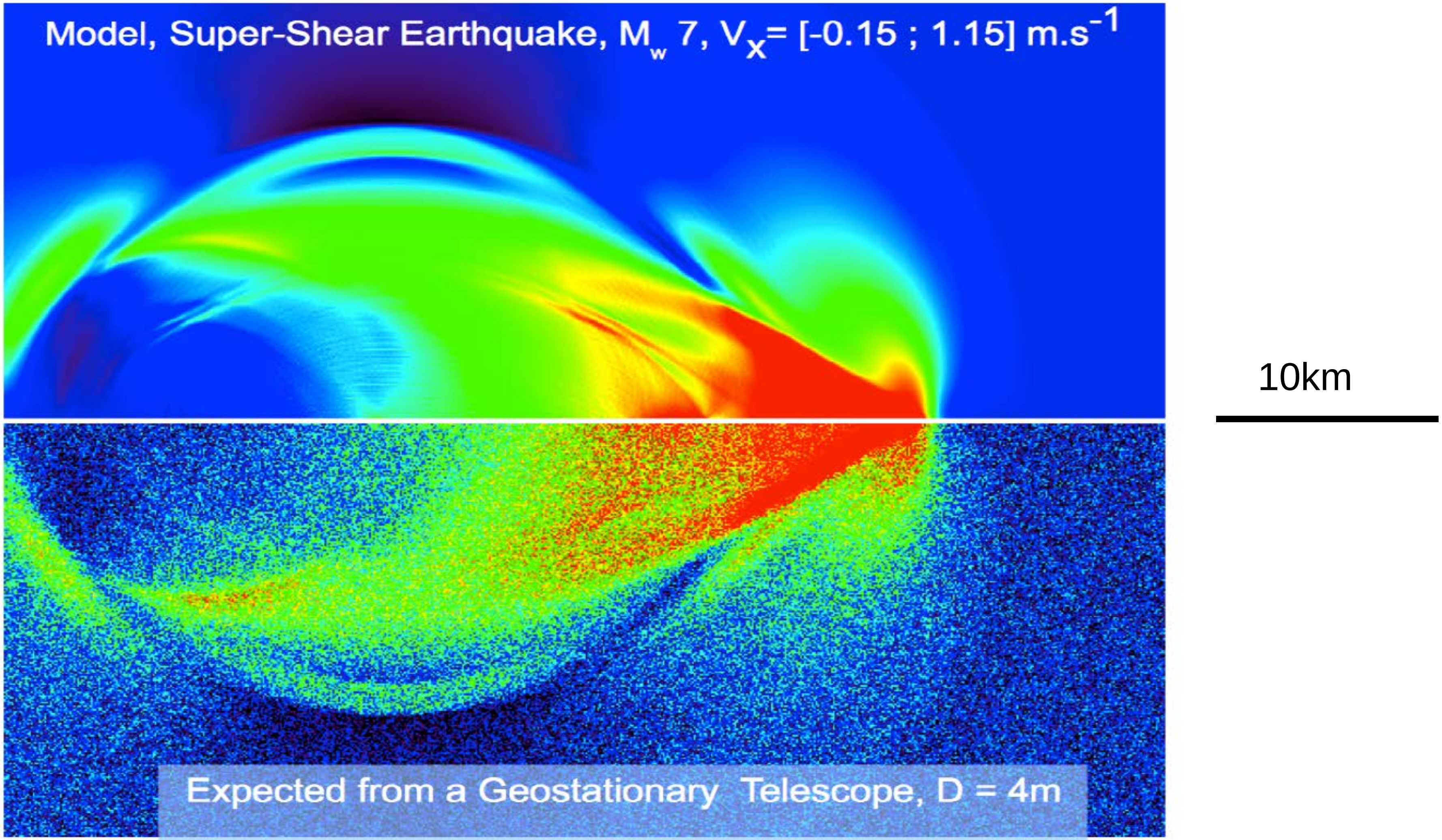

(Michel et al, 2012)

The ‘Shake Out’ scenario (a Mw 7.8 earthquake on the San Andreas Fault)

Simulation by Rob Graves, USGS(Graves et al., 2011)

A M_w 7.8 quake seen by a 3.6m GSI

Area simulated

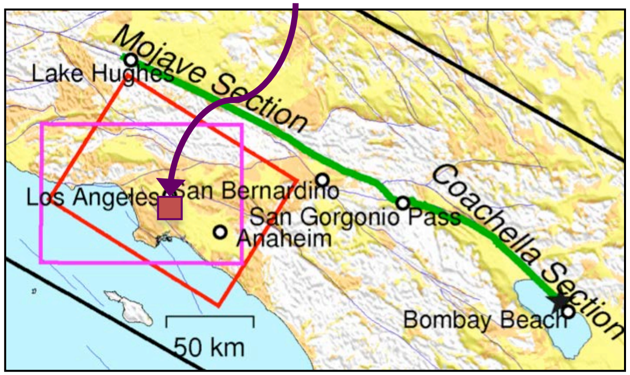

Unshifted Frame

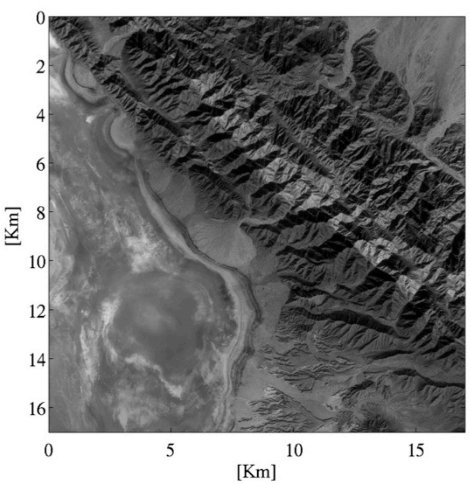

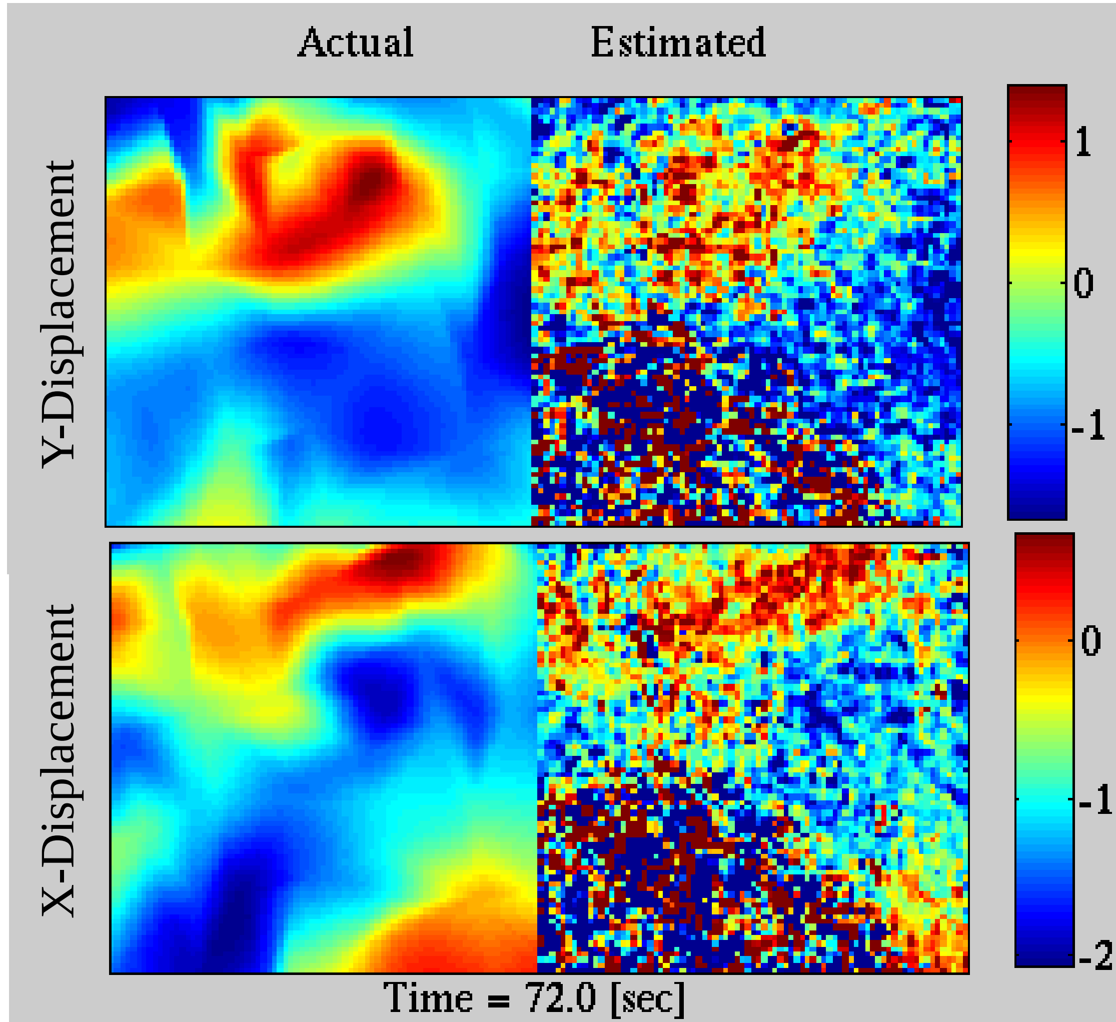

- Shakeout Sim: a M_v = 7.8 quake as seen by a 3.6m GSI

(Erkin Sidick, Dave Redding)

Ice

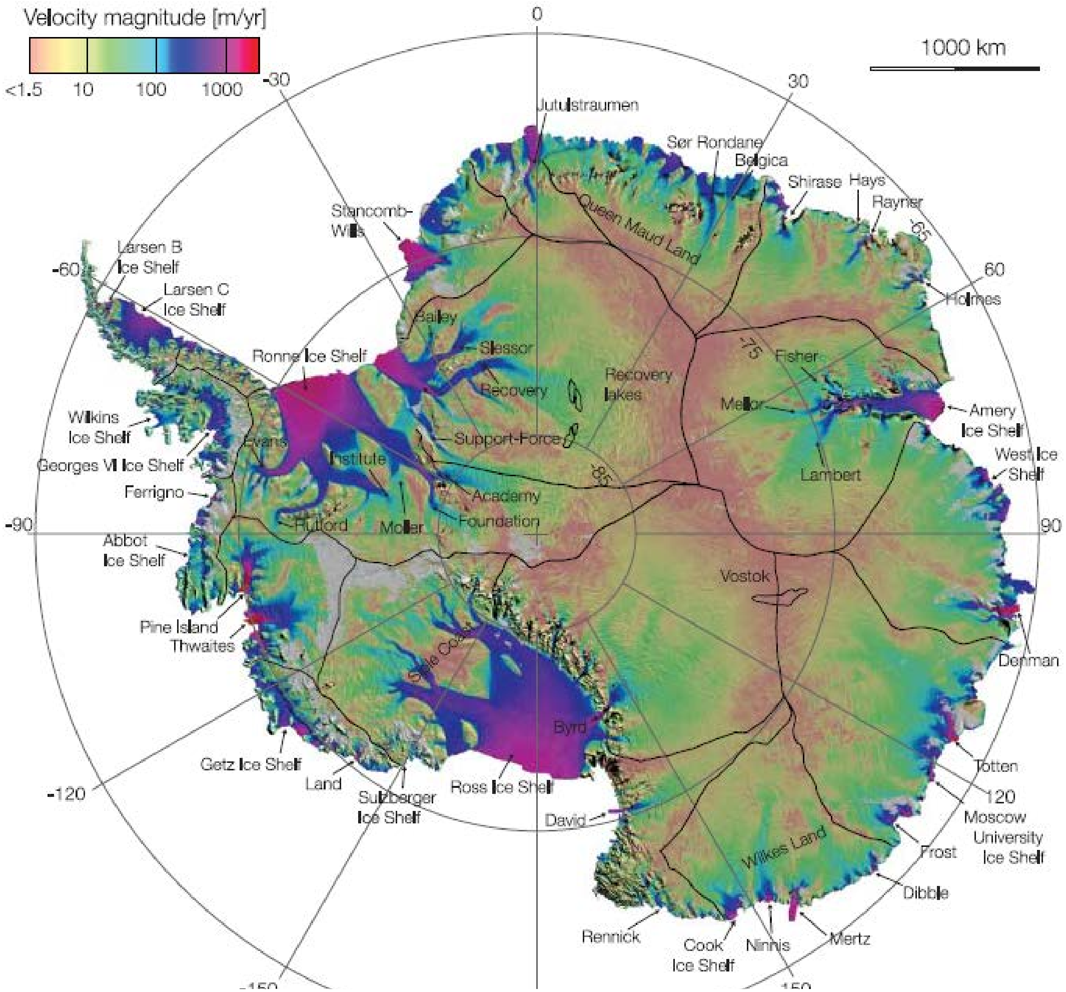

(Rignot et al., 2011)

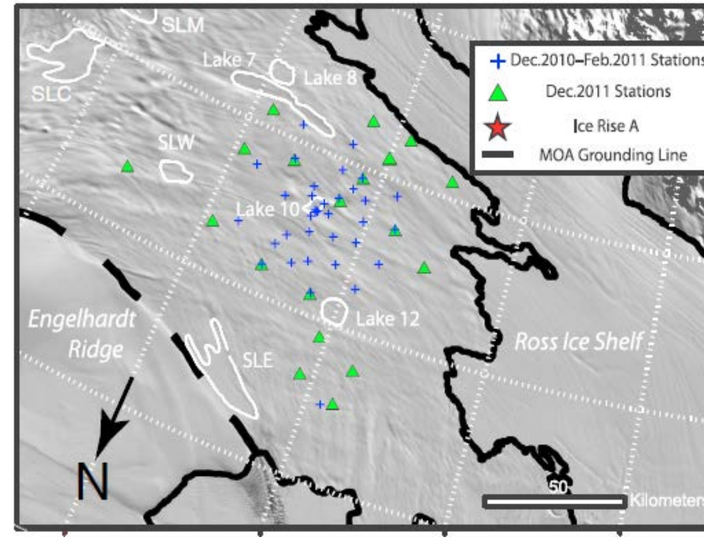

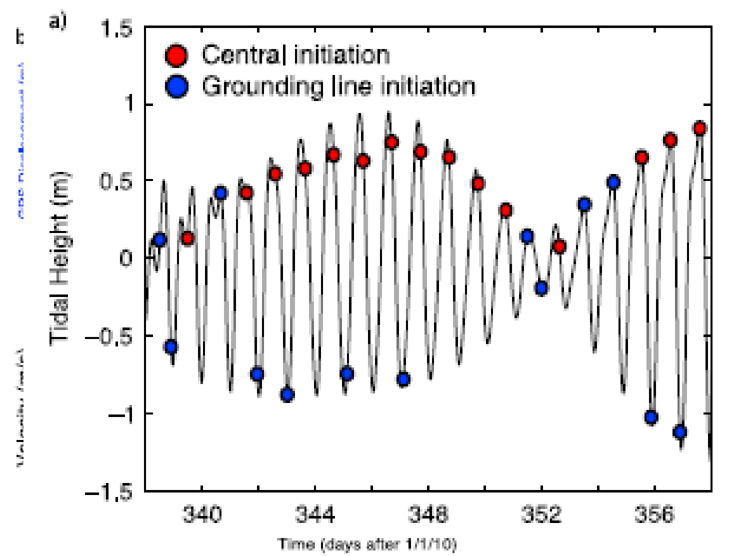

(Pratt et al, JGR, 2014)

Volcanoes

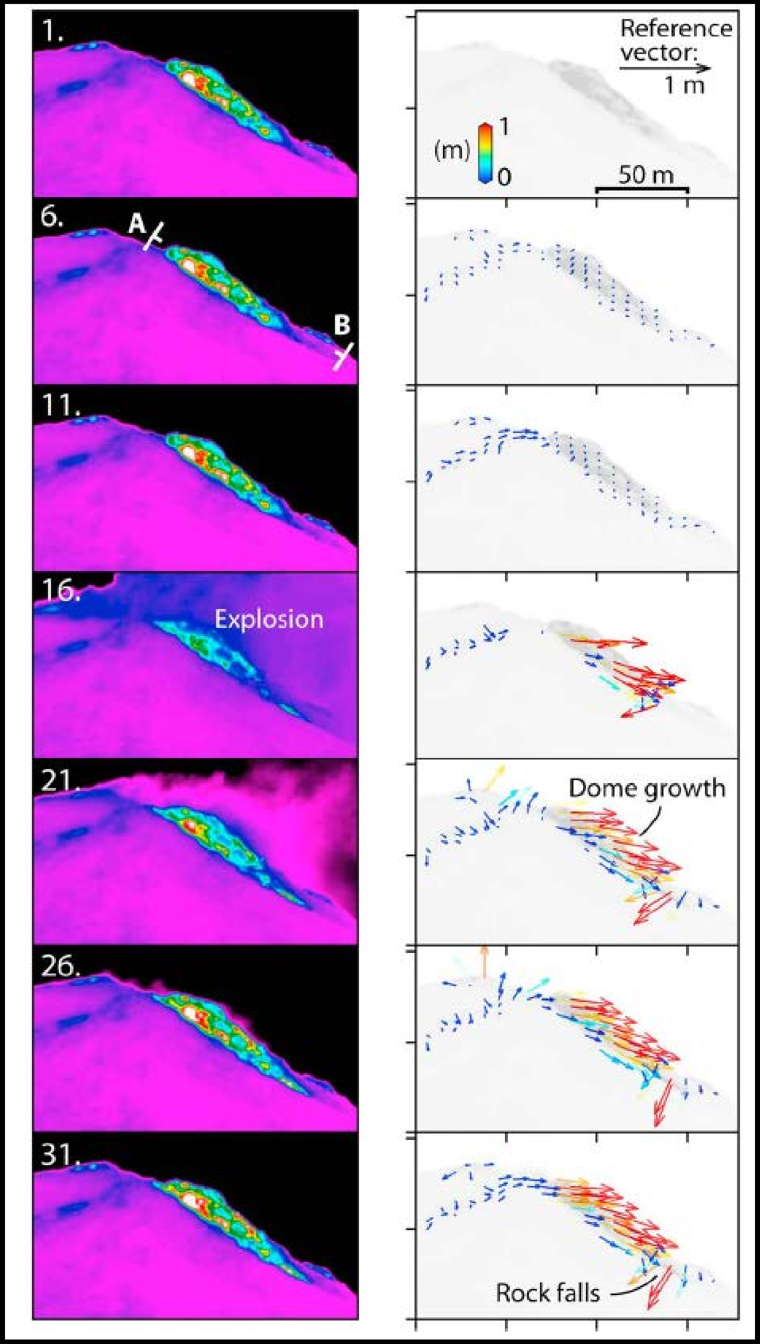

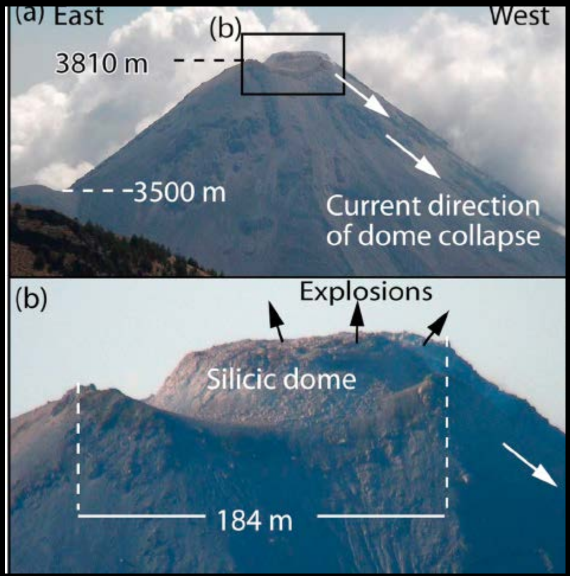

(Walter, JGR, 2013)

Volcanoes

(Johnson et al., Nature, 2008)

Thanks to collaborators:

CEA: Rémi Michel, Renaud Binet…

CALTECH: Sébastien Leprince, Francois Ayoub, Jiao Lin, Bruno Conejo, Sylavain Barbot, James Hollingsworth, Neus Sabater…

Jean-Paul Ampuero, Nadia Lapusta
Nathan Bridges, Dave Redding, Erkin Siddick…

and funders:

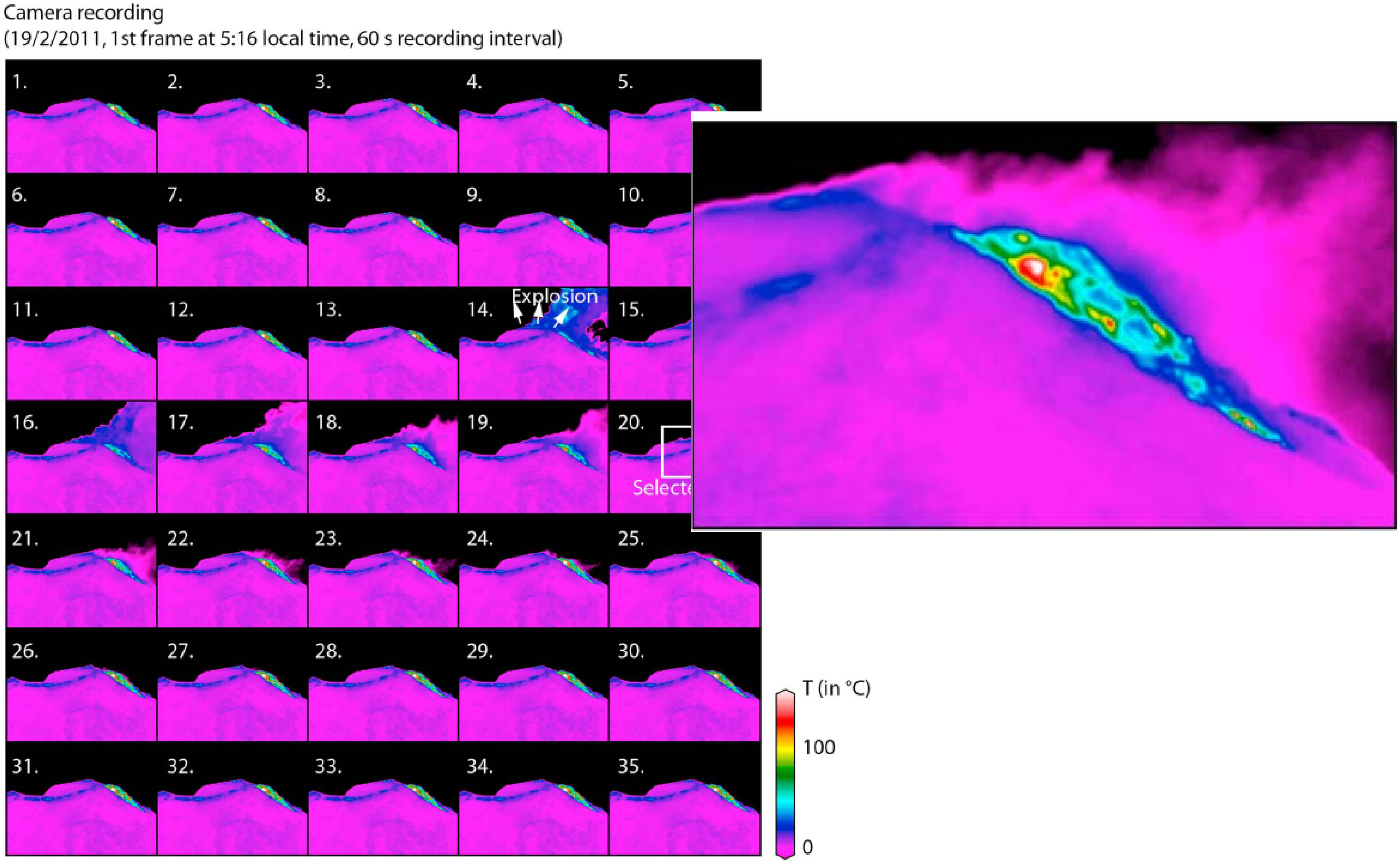

Figure 3. Thermal images of the summit region taken at night from a location north of the Volcán de Colima, 2.59 km from the northern rim of the summit crater. A subset of infrared time-lapse recordings enabled the retrieval of pixels with ~1 m^2 dimensions. This work employed digital image correlation methods to analyze systematic pixel offsets. The white box in frame 20 outlines the area shown in Figure 4. The thermal images shown here are saturated for visualization purposes only. Also shown is the approximate location and direction of explosions (the arrows in frame 14).

(Walter, JGR, 2013)

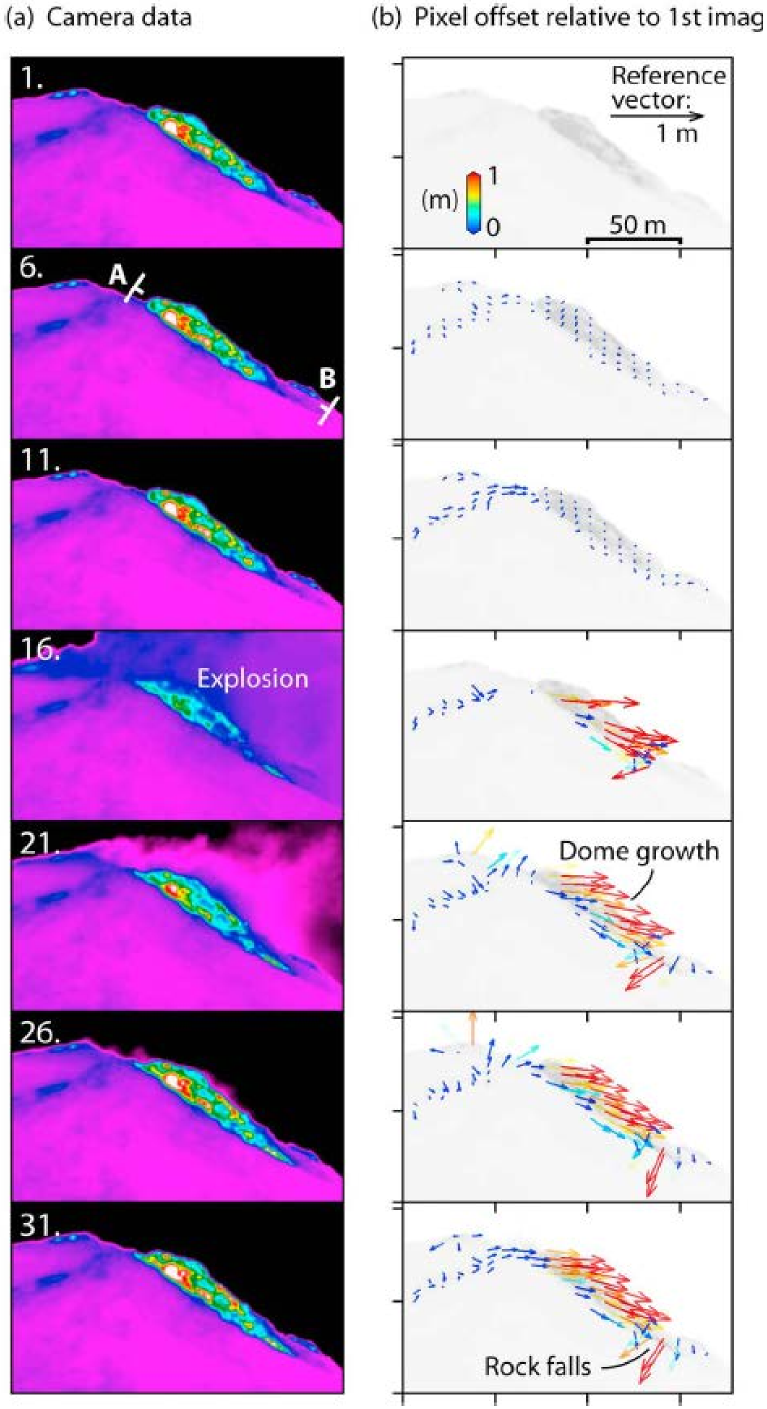

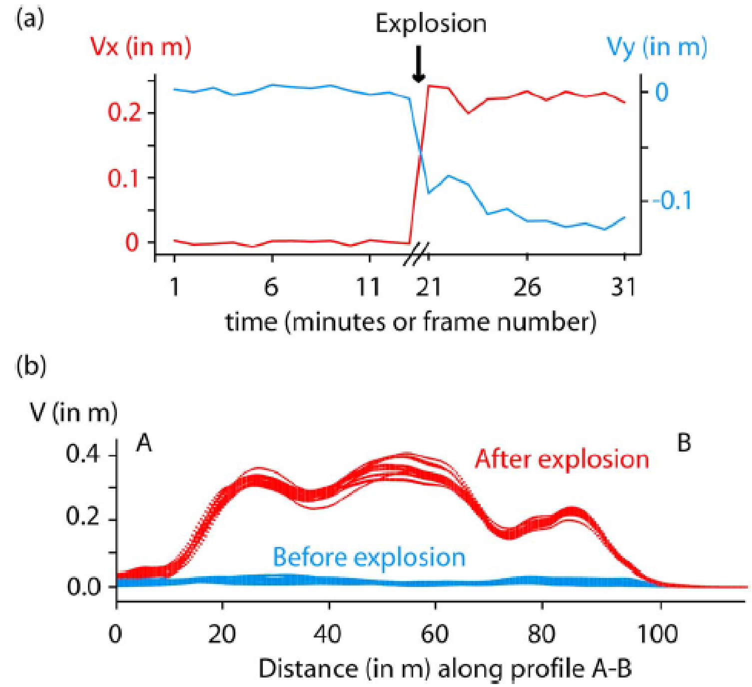

Figure 6. (a) Comparison of the mean horizontal (Vx) and vertical (Vy) displacements calculated for region RE1 (see Figure 4 for the location). The first image is the reference image, with which each subsequent image is cross-correlated. For visualization purposes, we show every fifth image only. Note the occurrence of a generally stepwise deformation without precursory deformation. Vx ends after the explosion, whereas Vy continues for up to ~10 min. (b) Displacement occurred along profile A-B, as indicated in frame 6 of Figure 4a. The largest displacement occurred at the center and above.

(Walter, JGR, 2013)

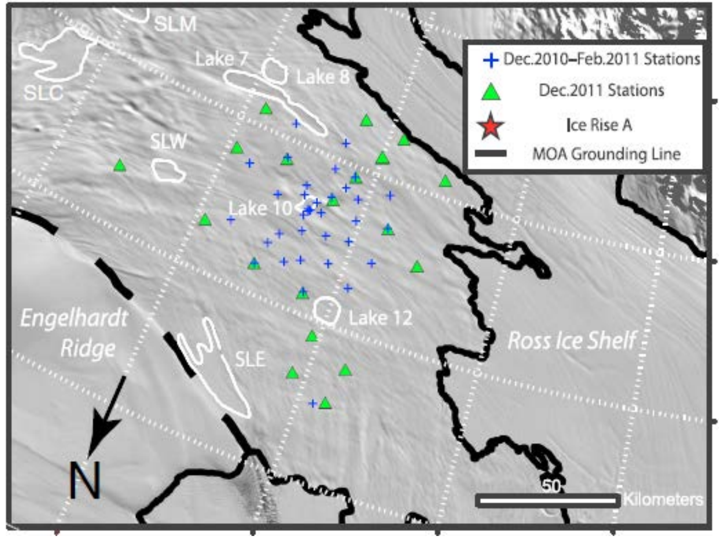

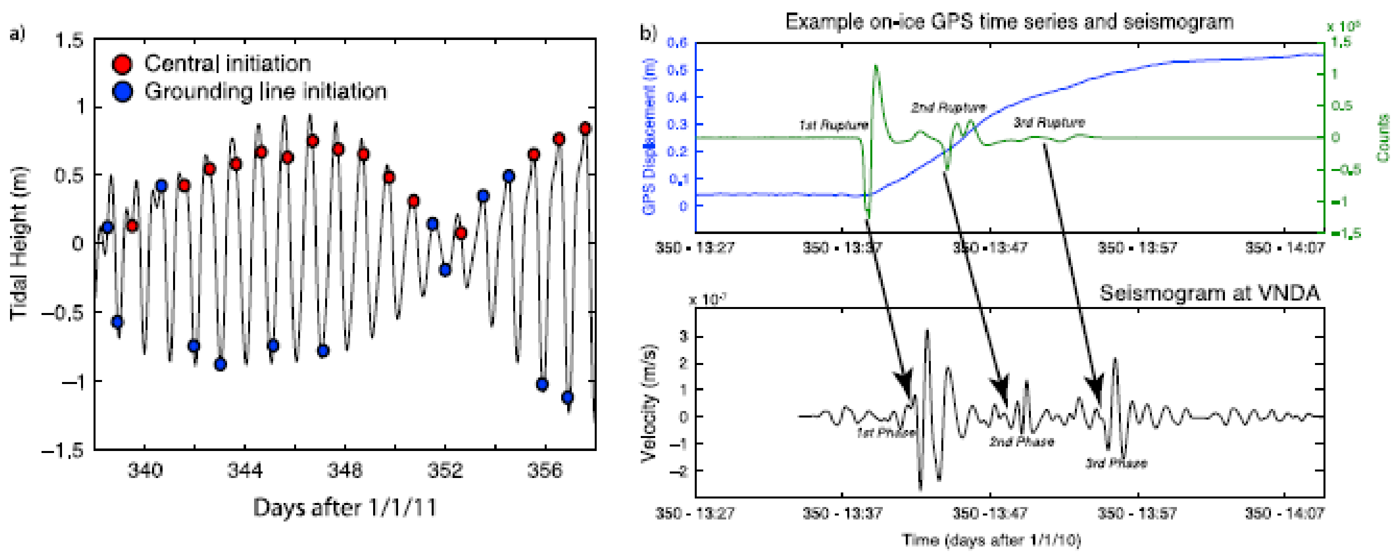

Figure 2. (a) Slip event times and types. Note that missed low-tide events are now more common than low-tide slips. Ross Sea tide (black) is CATs2008a tidal model (L. Padman, personal communication, 2008). (b) Example on-ice colocated GPS (blue) and raw seismogram (green—instrument response not removed) and the correlation with 30–100 s filtered vertical-component seismogram at VNDA showing the relationship of in situ translational velocity changes and far-field seismic phases.

(Pratt et al, JGR, 2014)

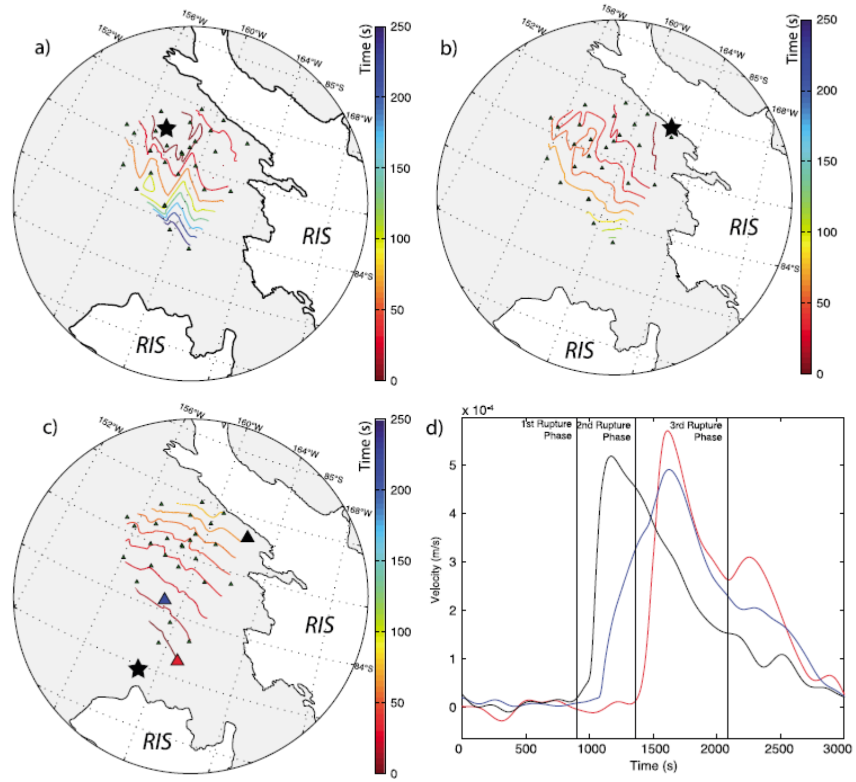

Figure 4. Rupture patterns using combined 2010 and 2011 traveltime pick data. The first rupture phase is recorded at all stations but two of the most downstream, whereas the second rupture phase is recorded at all stations. Similar slip events from both field seasons using duration and onset location were combined to show rupture propagation with isochrone contours for (a) central initiation, (b) grounding-line initiation, and (c) second-phase initiation. RIS = Ross Ice Shelf; black stars show acceleration initiation locations. (d) Broadband velocity functions formed by combining GPS and seismograph records for three stations across the array. Colors correspond to stations shown in Figure 4c. Vertical black lines show the onsets of accelerations that correspond to the teleseismic phases.

(Pratt et al, JGR, 2014)

1. The surface of Earth and other planet is the primary source of information on subsurface structures and geological history.

2. The surface of Earth and other planet changing as a result of both internal and external dynamic processes.

3. The volume of remote sensing data available is increasing exponentially, driven by commercial and defense applications.

4. Science opportunities have emerged also because of development of specific techniques to exploit those data.